

Discovery of Compounds Blocking the Proliferation of *Toxoplasma gondii* and *Plasmodium falciparum* in a Chemical Space Based on Piperidinyl-Benzimidazolone Analogs

Nadia Saïdani,^{a,b} Cyrille Y. Botté,^{a,c} Michael Deligny,^{d*} Anne-Laure Bonneau,^{d*} Janette Reader,^e Ronald Lasselin,^e Goulven Merer,^e Alisson Niepceron,^f Fabien Brossier,^f Jean-Christophe Cintrat,^d Bernard Rousseau,^d Lyn-Marie Birkholtz,^e Marie-France Cesbron-Delauw,^c Jean-François Dubremetz,^b Corinne Mercier,^c Henri Vial,^b Roman Lopez,^{d*} Eric Maréchal^a

Commissariat à l'Energie Atomique, Centre National de la Recherche Scientifique, Université Grenoble Alpes, Institut National de la Recherche Agronomique, Unité Mixte de Recherche 5168, Institut de Recherches en Technologies et Sciences pour le Vivant, Grenoble, France^a; Centre National de la Recherche Scientifique, Université Montpellier II, Unité Mixte de Recherche 5235, Montpellier, France^b; Centre National de la Recherche Scientifique, Université Grenoble Alpes, Unité Mixte de Recherche 5163, Institut Jean Roget, Grenoble, France^c; Commissariat à l'Energie Atomique, Institut de Biologie et Technologies de Saclay, Laboratoire de Chimie Bioorganique, Gif-sur-Yvette, France^d; Malaria Research Group, Department of Biochemistry, University of Pretoria, Pretoria, South Africa^e; Institut National de la Recherche Agronomique, Université de Tours, Unité Mixte de Recherche 1282, Infectiologie Animale et Santé Publique, Centre de Recherche de Tours, Nouzilly, France^f

A piperidinyl-benzimidazolone scaffold has been found in the structure of different inhibitors of membrane glycerolipid metabolism, acting on enzymes manipulating diacylglycerol and phosphatidic acid. Screening a focus library of piperidinyl-benzimidazolone analogs might therefore identify compounds acting against infectious parasites. We first evaluated the *in vitro* effects of (S)-2-(dibenzylamino)-3-phenylpropyl 4-(1,2-dihydro-2-oxobenzo[d]imidazol-3-yl)piperidine-1-carboxylate (compound 1) on *Toxoplasma gondii* and *Plasmodium falciparum*. In *T. gondii*, motility and apical complex integrity appeared to be unaffected, whereas cell division was inhibited at compound 1 concentrations in the micromolar range. In *P. falciparum*, the proliferation of erythrocytic stages was inhibited, without any delayed death phenotype. We then explored a library of 250 analogs in two steps. We selected 114 compounds with a 50% inhibitory concentration (IC₅₀) cutoff of 2 μM for at least one species and determined *in vitro* selectivity indexes (SI) based on toxicity against K-562 human cells. We identified compounds with high gains in the IC₅₀ (in the 100 nM range) and SI (up to 1,000 to 2,000) values. Isobole analyses of two of the most active compounds against *P. falciparum* indicated that their interactions with artemisinin were additive. Here, we propose the use of structure-activity relationship (SAR) models, which will be useful for designing probes to identify the target compound(s) and optimizations for monotherapy or combined-therapy strategies.

The phylum *Apicomplexa* comprises a group of unicellular eukaryotes, including obligate intracellular parasites that cause diseases ranging from benign to serious (1). In humans, the most devastating of these infections is malaria, caused by *Plasmodium* parasites, with *Plasmodium falciparum* being the deadliest. Malaria affects about 225 million humans and results in 650,000 deaths every year (2). *Toxoplasma gondii* is another *Apicomplexa* organism that causes toxoplasmosis, affecting one-third of the world population (3). Other parasites, such as *Babesia* spp., *Neospora* spp., and *Eimeria* spp., cause diseases of veterinary importance (4). *Apicomplexa* require large amounts of glycerolipids to build up membrane compartments throughout their life cycle. *Plasmodium* asexual proliferation illustrates this demand. Once invading a hepatocyte, a single sporozoite divides, producing 40,000 merozoites (5). Each merozoite then begins a cycle of schizogonic development inside erythrocytes. As a consequence, a 500 to 700% increase in membrane lipids is observed in infected erythrocytes compared to uninfected ones (6).

The structure of glycerolipids is obtained by the assembly of (i) a 3-carbon glycerol backbone originating from glycerol-3-phosphate (G3P), (ii) fatty acids (FA) esterified at positions *sn* -1 and *sn* -2 in glycerol, and (iii) a polar head at position *sn* -3. It has long been considered that *Apicomplexa* scavenge their fatty acids and glycerolipids from the host (5–8). However, the existence of biosynthetic pathways has been demonstrated, leading to the consensus that *Apicomplexa* meet their actual demand by a combination of scavenging and *de novo* synthesis (9).

The synthesis of glycerolipids is initiated by two acyltransferases generating lysophosphatidic acid (LPA) and phosphatidic acid (PA) (Fig. 1). LPA can be synthesized in the endoplasmic reticulum (ER) by an acyl-CoA:G3P acyltransferase (CoA, coenzyme A) in both *P. falciparum* (10) and *T. gondii*. Genes encoding acyl-CoA:1-acyl-G3P acyltransferases, which catalyze the synthesis of PA in the ER, have been predicted at least in *T. gondii*. Alternatively, PA might be neosynthesized in the apicoplast in both *P. falciparum* and *T. gondii* (11). The second main precursor for glycerolipid synthesis is diacylglycerol (DAG) (Fig. 1), which is

Received 5 July 2013 Returned for modification 15 October 2013

Accepted 8 February 2014

Published ahead of print 18 February 2014

Address correspondence to Eric Maréchal, eric.marechal@cea.fr.

N.S. and C.Y.B. contributed equally to this article.

* Present address: Michael Deligny, UCB Pharma, Brussels, Belgium; Anne-Laure Bonneau, Institut National de la Propriété Industrielle, Courbevoie, France; Roman Lopez, Taj-Deloitte, Paris, France.

This article is dedicated to the memory of our coauthor Fabien Brossier, who sadly passed away in January 2014. We express our deepest condolences to his family, friends, and colleagues at INRA Tours.

Supplemental material for this article may be found at <http://dx.doi.org/10.1128/AAC.01445-13>.

Copyright © 2014, American Society for Microbiology. All Rights Reserved.

doi:10.1128/AAC.01445-13

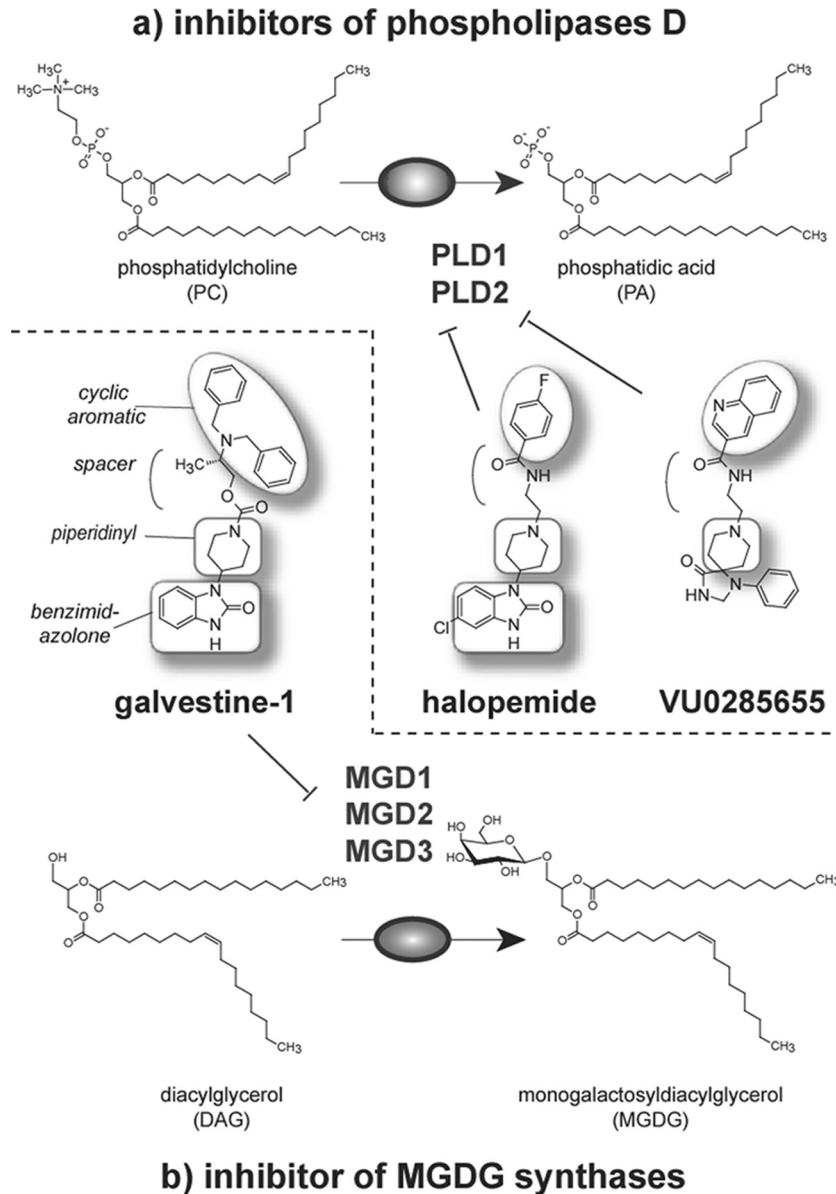


FIG 1 Piperidinyl-benzimidazolones acting on glycerolipid metabolism. Independent reports have shown that 4-(2-oxo-3H-benzimidazol-1-yl)piperidine-1 (or piperidinyl-benzimidazolone) analogs inhibit specifically glycerolipid-manipulating enzymes. (a) Chemical structures of halopemide (PubChem ID CID 65490) and VU0285655. *N*-[2-[4-(5-chloro-2-oxo-3H-benzimidazol-1-yl)piperidine-1-yl]ethyl]-4-fluorobenzamide was shown to selectively inhibit mammal phospholipases D (in humans, PLD1 and PLD2) (41, 42). An exploration of the chemical space of halopemide analogs has shown that compounds can be equally efficient on PLD1 and PLD2 or more specific to one or the other. Halopemide and halopemide analogs therefore inhibit the conversion of PC into PA. Compounds with a 1-phenyl-1,3,8-triazaspiro[4,5]decan-4-one scaffold, such as VU0285655 (PubChem ID CID 44138050), exhibit a higher selectivity for PLD2 (42, 43). (b) Chemical structure of galvestine-1. [(2S)-2-(dibenzylamino)propyl] 4-(2-oxo-3H-benzimidazol-1-yl)piperidine-1-carboxylate (PubChem ID CID 25192811) was shown to selectively inhibit plant MGDG synthases (three isoforms in *A. thaliana*, MGD1, MGD2, and MGD3) by competition with DAG (23, 40).

neosynthesized by the hydrolysis of PA by a phosphatidate phosphatase (PAP). At least two genes are predicted to encode PAPs in *P. falciparum* and *T. gondii*. Conversely, DAG can be phosphorylated into PA by diacylglycerol kinases (DGK) in both *P. falciparum* and *T. gondii*. PA and DAG can also be generated from existing phospholipids via the action of phospholipase D (PLD) and phospholipase C (PLC), respectively. Although PLDs and PLCs are widely represented in eukaryotes, only one gene has been demonstrated to encode a PLC in *P. falciparum* (12) and *T. gondii* (13). To our knowledge, no PLD has been characterized in any *Apicomplexa* parasite.

DAG and PA serve as precursors for all membrane glycerolipids. In eukaryotes, two main subcellular compartments are responsible for the synthesis of complex glycerolipids: one is the ER, synthesizing phospholipids, and the other one is the plastid of photosynthetic organisms, synthesizing nonphosphated glycerolipids, including monogalactosyldiacylglycerol (MGDG). Although the apicoplast derives from a photosynthetic plastid (14), no enzyme synthesizing glycerolipids was identified in this organelle (15, 16).

Given the importance of glycerolipids for membrane biogenesis, their metabolism appears to be a potential target for novel treatments. Taking the available data summarized above, the bio-

synthesis of glycerolipids is therefore constituted of 3 metabolic segments: (i) the neosynthesis/scavenging of FAs, (ii) the PA↔DAG hub, and (iii) the synthesis of phospholipids from PA and DAG. In the first metabolic segment, the synthesis of FAs in the apicoplast by FA synthase (FAS) II has inspired numerous attempts to develop novel drugs (for a review, see 9 and 17), but erythrocytic stages of *P. falciparum* were shown to survive without a functional *de novo* synthesis (5, 18, 19), and the efficacy of anti-FAS II drugs against the blood stages is likely due to off-target effects (9). In the third metabolic segment, the synthesis of glycerophospholipids, and particularly phosphatidylcholine, was shown to be a valid target: chemical scaffolds like thiazolium analogs of choline (20, 21) or phospholipid structural analogs, like PG12 (22), have been proposed to be novel classes of efficient antiparasitic drugs. No drug has been developed to target the second metabolic segment, i.e., at the level of the PA↔DAG hub. In this article, we explore the chemical space of piperidinyl-benzimidazolone analogs of galvestine-1 (a competitor of DAG binding on MGDG synthases) and halopemide (an inhibitor of PLDs producing PA) (Fig. 1) to search for novel classes of compounds acting on the proliferation of *T. gondii* and *P. falciparum*.

MATERIALS AND METHODS

Library of piperidinyl-benzimidazolone analogs. The library used in this work was described previously (23). The structures are given in Table S1 in the supplemental material. The compounds were synthesized and analyzed by liquid chromatography and nuclear magnetic resonance (NMR). High-pressure liquid chromatography was performed using a Waters system (2525 binary gradient module, in-line degasser, 2767 sample manager, and 2996 photodiode array detector). Analytical reverse-phase (RP) high-pressure liquid chromatography (HPLC) was achieved with an X-bridge C₁₈ column (100 by 4.6 mm, 3.5- μ m particle size, and 135- Å pore size) at a 1-ml/min flow rate. Preparative RP-HPLC was achieved with an X-bridge C₁₈ column (150 by 19 mm, 5- μ m particle size, and 135- Å pore size) at a 17-ml/min flow rate. Elution was carried out with a gradient of A (99.9% water/0.1% HCOOH) and B (99.9% acetonitrile [ACN]/0.1% HCOOH). Mass spectra were obtained on a Waters Micromass ZQ system with a ZQ2000 quadrupole analyzer. The ionization was performed by electrospray with a source temperature of 120°C, a cone voltage of 20 V, and continuous sample injection at a 0.3-ml/min flow rate. Mass spectra were recorded in positive ion mode in the *m/z* 100 to 2,000 range and treated with the MassLynx 4.0 software. NMR experiments were performed on a Bruker Avance 400 Ultrashield (Karlsruhe, Germany). The spectra were recorded at room temperature at 400 MHz for ¹H NMR and 100 MHz for ¹³C. The samples were dissolved in cyclohexane-ethyl acetate (7:3 [vol/vol]) at a concentration of 5 mM. The chemical shifts are given in ppm and the coupling constants in Hz. (Chemical characterizations and commercial sources are given in the supplemental material for a subset of compounds analyzed more carefully than described here.) The average purity is 93.34% (minimum to maximum, 90 to 99). In accordance with the Lipinski rules, the compounds had, on average, 0.86 H-bond donors (minimum to maximum, 0 to 4), 4.47 H-bond acceptors (minimum to maximum, 2 to 9), an average molecular weight of 537 (minimum to maximum, 217 to 844), and an average logP of 5.18 (minimum to maximum, 0.47 to 9.71). All compounds were solubilized in dimethyl sulfoxide (DMSO) and stored at -20°C until use.

***T. gondii* culture in human foreskin fibroblasts.** *T. gondii* RH and RH- β 1 strains were maintained by serial passages in a confluent human foreskin fibroblast (HFF) monolayer, as described previously (24, 25). The RH- β 1 strain carries the *Escherichia coli lacZ* (β -galactosidase) gene under the control of the SAG1 promoter (26). The cultures were maintained in Dulbecco's modified Eagle medium (DMEM) containing L-glutamine supplemented with 10% fetal bovine serum (FBS) and antibiotics

(10,000 U · ml⁻¹ penicillin and 10 mg · ml⁻¹ streptomycin) (Gibco, Invitrogen Corporation, United Kingdom) at 37°C with 5% CO₂. Imaging was performed using an Axioplan 2 microscope and an AxioCam MRn camera (Zeiss).

***In vitro* assay of *Toxoplasma* proliferation by colorimetric titration.** Microtiter plates (96 wells) were seeded with HFF cells and allowed to grow to confluence in DMEM containing L-glutamine, 10% FBS, and antibiotics (10,000 U · ml⁻¹ penicillin, 10 mg · ml⁻¹ streptomycin) at 37°C with 5% CO₂. *T. gondii* cells used in the 50% inhibitory concentration (IC₅₀) assay were prepared as follows: a culture of RH- β 1 that had completely lysed HFF monolayers was forced through a 27-gauge needle twice and then filtered through a 3- μ m-pore-size filter. The flowthrough was centrifuged at 250 × *g* for 10 min to collect the parasites, which were washed once in 5 ml phosphate-buffered saline (PBS). The parasites were resuspended in PBS and counted (25). HFF cell monolayers grown in 96-well microtiter plates were infected with 10⁴ parasites per well (200 μ l) and incubated on ice for 15 min to allow parasite sedimentation and promote synchronization for invasion. The parasites were allowed to invade for 15 min at 37°C with 5% CO₂. The wells were rinsed three times with PBS. Intracellular parasites were allowed to grow in the absence (controls) or presence of a range of compound concentrations (1 nM to 500 μ M). The controls were grown in DMEM with or without DMSO. Each assay was carried out in triplicate. The plates were incubated at 37°C with 5% CO₂ for 48 to 72 h to allow parasite development until the control wells were fully lysed (27). The β -galactosidase activity was measured as described earlier (26). The plates were read at 570 and 630 nm on a Bio-Tek microtiter plate reader. The results are presented as the mean \pm 2 standard errors of the mean. Triplicates of the standard curve experiments were carried out in parallel by infecting another 96-well plate with serial dilutions of the corresponding parasite strain (0 to 10⁷ parasites/well).

***Toxoplasma* motility assay.** The assay is based on the deposition of surface proteins (SAG1) after the gliding of *T. gondii* on a glass slide (28). Glass slides were coated with poly-D-lysine (10 μ g · ml⁻¹ in PBS) for 1 h at 37°C and washed with PBS. Freshly purified tachyzoites (10⁷) were preincubated with or without the tested compound and deposited onto the surface of a coated slide. After 10 min at room temperature, the excess liquid was removed, 500 μ l of poly-D-lysine (10 μ g · ml⁻¹ in D10 medium) was added, and the slide was incubated for 25 min at 37°C. The gliding trails were visualized by immunofluorescence using an anti-SAG1 antibody (29, 30) at 1:500, followed by a 45-min incubation with a Texas Red coupled goat anti-mouse IgG (H+L) (1:1,000; Molecular Probes; Invitrogen). The labeled gliding trails were visualized using an epifluorescence Axioplan 2 microscope (Zeiss) after excitation at 596 nm and capture of emission at 620 nm, using an AxioCam MRn camera (Zeiss).

***Toxoplasma* apical complex integrity.** The apical complex integrity was concisely assayed by analyzing the *in vitro* induction of the extrusion of the conoid by Ca²⁺ ionophores and the secretion of MIC2 by micronemes induced by ethanol. For the conoid extrusion assay, 10⁵ freshly purified tachyzoites were preincubated with or without the tested compound and incubated with 1 μ M ionomycin, as described earlier (31). To test the ethanol-induced secretion of MIC2, 10⁹ freshly purified tachyzoites were preincubated with or without tested compound, washed three times with PBS, and suspended in FBS 0.1% in PBS (pH 7.4). Ethanol was added at a 1% final concentration, and the parasites were incubated for 1 h at 37°C (32). The parasites were then separated from the microneme content by centrifugation at 2,000 × *g*. The supernatant was collected and analyzed by SDS-PAGE, electrotransfer, and Western blotting using anti-MIC2 antibodies (monoclonal antibody [MAb] T3.4A11.2b4; 1:5,000 dilution) and a secondary mouse antibody coupled with peroxidase and revealed by chemiluminescence (ECL kit; Millipore). The anti-GRA1 antibody (MAb Tg17.43.1; 1:5,000 dilution) (33) was used as a control.

***P. falciparum* culture.** Experiments were performed using chloroquine-sensitive (3D7 and Nigerian) or chloroquine-resistant (W2, FCM29, and Dd2) *P. falciparum* strains, as indicated in Results. For sys-

tematic screening, we used the 3D7 strain. The strains were maintained in continuous culture in human erythrocytes, according to the method of Trager and Jensen (34).

Standard evaluation of *in vitro* antimalarial activity. *In vitro* antimalarial activity was measured using asynchronous 3D7 chloroquine-sensitive *P. falciparum*-infected red blood cells (RBC). Suspensions of infected RBC at 1.5% final hematocrit and 0.6% parasitemia were cultured in complete medium (RPMI 1640 complemented with 25 mM HEPES [pH 7.4] and 0.5% AlbuMAX I) in the absence (controls) or presence of compounds, according to the procedure outlined by Desjardins et al. (35). The compounds were dissolved in DMSO at 10 mM and then diluted in culture medium so that the final DMSO concentration was never >0.5%. After a 48-h (length of the parasite's cycle) or 96-h incubation (as indicated in Results), 0.5 μ Ci [3 H]hypoxanthine was added to each well. After 18 h of incubation at 37°C, the cells were lysed, and the parasite macromolecules, including radioactive nucleic acids, were retained on glass fiber filters. Emissions from the radiolabeled material were counted (Tri-Carb 2900TR scintillation counter). The radioactive background was obtained after incubation of noninfected red blood cells under the same conditions. Analyses of dose-effect curves were performed with the GraphPad Prism analytical software. The drug effects were expressed as the IC₅₀ values. The results are the means of at least two independent experiments (different cell cultures and different compound dilution stocks), each performed in duplicate.

Drug effects during the *P. falciparum* erythrocyte cycle. The parasites were synchronized twice by 5-min treatments with sorbitol 5% and washing with RPMI, a process allowing for the selection of ring stages. Infected RBC (1% final hematocrit, 0.6% parasitemia, 1.5 ml) were then grown in presence or absence of compounds. To evaluate the effects at different stages of the parasitic cycle, the compounds were added at 4 h for the ring stage, 20 h for the trophozoite stage, or 32 h for the schizont stage (following the second sorbitol treatment). After 4 h of incubation with the compounds, the parasites were washed and resuspended in fresh medium without drugs. At 52 h, 0.5 μ Ci [3 H]hypoxanthine was added. The reactions were stopped at 75 h by freezing the plate at -80°C, and the cells were lysed and filtered as described above to determine the IC₅₀s of the compounds.

Isobolograms for the evaluation of interactions between selected compounds and artemisinin against *P. falciparum*. To examine the *in vitro* interaction of compounds 8 and 12 with artemisinin, isobolograms were constructed as described earlier (36). Concentrations of each compound were expressed as fractional inhibitory concentrations (FIC), which is the fraction of IC₅₀ of a compound when tested alone. The isobolograms were constructed by plotting the FIC for the tested compounds versus the FIC for artemisinin. A drug combination is considered synergistic if the sum of the two FIC values for a given combination (Σ FIC) is <0.5 or antagonistic when the Σ FIC is >2 (37) or 4 (38, 39). The nature of the interaction between drugs with Σ FIC values between 0.5 and 2 (or 4) should be considered indifferent (38), i.e., simply additive.

***In vitro* effects of compounds on human cells.** Human lymphoblasts (Jurkat), erythroblasts (K-562), monocytes (THP-1), and macrophages (U-937) were seeded in 200 μ l in complete medium (RPMI 1640 complemented with 10% fetal calf serum [FCS], 1% glutamine, 1% penicillin-streptomycin) in 96-well microplates (8,000 cells per well) and incubated 24 h at 37°C and 5% CO₂ in the presence of various concentrations of the tested molecules. [3 H]Thymidine (0.5 μ Ci) was then added, followed by a supplementary incubation of 6 h. The reaction was stopped by congelation at -80°C. Radioactive incorporations into nucleic acids were measured by scintillation counting after collection on glass fiber filters. Radioactive background was measured from complete medium and subtracted from each corresponding well. The IC₅₀ is the drug concentration that led to 50% cell growth inhibition. In the case of human hepatocellular liver carcinoma cells (HepG2), the cells were seeded in DMEM (supplemented with 10% [vol/vol] heat-inactivated FBS and 1% penicillin-streptomycin at 37°C, 5% CO₂, 90% humidity, and 10⁵ cells per well) and grown for 24

h at 37°C in the presence of various concentrations of tested molecules. Cell viability was measured using the lactate dehydrogenase (LDH) assay (BioVision) by transferring 10 μ l of the supernatant to a new 96-well plate and adding 100 μ l LDH reaction mix (BioVision), incubation for 30 min at room temperature, and measuring the LDH activity through absorbance at 450 nm. Cell viability was expressed as a percentage of the control. Analyses of dose-effect curves were performed with the GraphPad Prism analytical software. The IC₅₀ values were graphically determined from at least two independent experiments (different cell cultures and different compound dilution stocks) performed in duplicate.

RESULTS

Selection of the library of piperidinyl-benzimidazolone analogs. Independent studies have shown that analogs of 4-(2-oxo-3H-benzimidazol-1-yl)piperidine-1 (or piperidinyl-benzimidazolone) might specifically inhibit DAG- or PA-manipulating enzymes. On one hand, [(2S)-2-(dibenzylamino)propyl] 4-(2-oxo-3H-benzimidazol-1-yl)piperidine-1-carboxylate (or galvestine-1; PubChem ID CID 25192811) was shown to selectively inhibit plant MGDG synthases (3 isoforms in *Arabidopsis thaliana*, MGD1, MGD2, and MGD3) by competition with DAG (23, 40) (Fig. 1). On the other hand, *N*-(2-(4-(5-chloro-2-oxo-1-benzimidazol-1-yl)piperidin-2-yl)ethyl)-*p*-fluorobenzamide (or halopemide; PubChem ID CID 65490) was shown to selectively inhibit mammalian phospholipase D enzymes (in humans, PLD1 and PLD2) (41, 42) (Fig. 1). Inhibition studies of truncated PLD1 support that halopemide analogs act by direct binding to the catalytic site, in which phosphatidylcholine (PC) is hydrolyzed into PA. An exploration of the chemical space of halopemide analogs further showed that compounds were equally efficient on PLD1 and PLD2 or more specific to one or the other. Thus, compounds with a 1-phenyl-1,3,8-triazaspiro[4,5]decan-4-one scaffold, like VU0285655 (PubChem ID CID 44138050), exhibit a higher selectivity for PLD2 (42, 43). Chemical tuning of the piperidinyl-benzimidazolone scaffold can therefore determine the target specificities of the obtained small molecules.

Based on (i) the central roles of DAG and PA in membrane glycerolipid metabolism and function, (ii) the evidence that piperidinyl-benzimidazolone analogs might compete with DAG or bind to the catalytic site of PLD for PC hydrolysis into PA, and (iii) the idea to use halopemide analogs for therapeutic purposes, we designed a library of 250 compounds to explore analogs of piperidinyl-benzimidazolone (structures are shown in Table S1 in the supplemental material). We searched for compounds that might interfere with the enzymes of glycerolipid metabolism, which manipulate the DAG-PA structure. The design of the library is based on chemical substitutions at the level of four diversification points in the structure of the molecules. These diversification points were termed "A" for the benzimidazolone end, "B" for the piperidinyl part, "C" for the substituted di-/tribezylamino ethoxy end, and "spacer" for the initial carboxylate segment between B and C (Fig. 2a). Figure 2 illustrates some families of compounds from this library, allowing testing features responsible for selectivity in galvestine-1, halopemide, and VU0285655. One family was designed to contain only the A1B1 scaffold shared by galvestine-1 and halopemide, including some compounds, like 5 and 6, with part C designed after that of VU285655 (Fig. 2b). Another family contains analogs whose structure contains a B1C1 structure, as found in galvestine-1, with substitutions at the C domain, i.e., the 4-(2-oxo-3H-benzimidazol-1-yl)piperidine-1 part (Fig. 2c). Other families of compounds are characterized by parts A and B

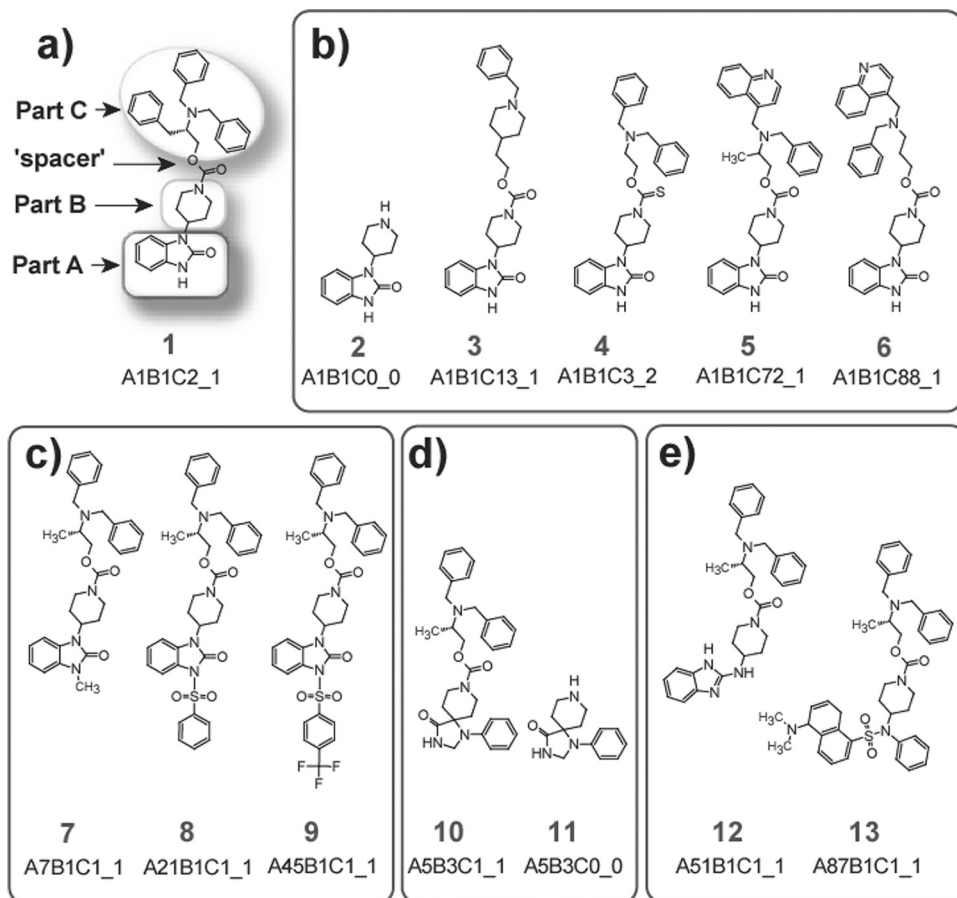


FIG 2 Illustration of compounds in the selected library of piperidinyl-benzimidazolone analogs. (a) Regions of the chemical structure subjected to variations. The chemical structures in the library have been dissected in four parts, illustrated on compound 1: “A” for the benzimidazolone end, “B” for the piperidinyl part, “C” for the substituted di/tribenzylamino ethoxy end, and “spacer” for the initial carboxylate segment between B and C. (b) Examples of compounds with a nonsubstituted 4-(2-oxo-3H-benzimidazol-1-yl)piperidine-1. Compound 2 represents the minimal structure. Compound 3 contains a part C shared with haloperamide. Compounds 5 and 6 contain a part C designed after that of VU285655. (c) Examples of compounds (7 to 9) with substitution at the level of 4-(2-oxo-3H-benzimidazol-1-yl)piperidine-1. (d) Examples of compounds (10 and 11) with parts A and B containing 1-phenyl-1,3,8-triazaspiro[4,5]decan-4-one scaffold also found in the structure of VU0285655. (e) Examples of compounds (12 and 13) with strong changes in parts A and B. All compounds are identified by an A#B#C#_# nomenclature following initial syntheses of compounds in the library. All structures of the library are shown in Table S1 in the supplemental material.

containing 1-phenyl-1,3,8-triazaspiro[4,5]decan-4-one scaffold, like VU0285655 (Fig. 2d), and compounds with significant changes in parts A and B (Fig. 2e).

In vitro analysis of (S)-2-(dibenzylamino)-3-phenylpropyl 4-(1,2-dihydro-2-oxobenzo[d]imidazol-3-yl)piperidine-1-carboxylate (compound 1) on *T. gondii*, *P. falciparum*, and human cells. (i) **In vitro effects of compound 1 on *T. gondii* tachyzoites.** To investigate whether piperidinyl-benzimidazolones might possess pharmacological potential against *Apicomplexa*, we initially tested galvestine-1 and an analog, (S)-2-(dibenzylamino)-3-phenylpropyl 4-(1,2-dihydro-2-oxobenzo[d]imidazol-3-yl)piperidine-1-carboxylate (compound 1) before exploring a more complete library. The compounds were assessed against *T. gondii* and *P. falciparum*. Both compounds inhibited the *in vitro* proliferation of *T. gondii* and *P. falciparum* with IC_{50} s of <15 μ M. The most potent inhibitor was compound 1, inhibiting *T. gondii* proliferation with an $IC_{50Toxoplasma}$ of 4.8 μ M (Fig. 3a) and *P. falciparum* with an $IC_{50Plasmodium}$ of 1.45 μ M (Fig. 3c). We then decided to perform a preliminary investigation of the mechanism of action of compound 1 on parasites and the potential cytotoxicity to human cells *in vitro*.

Figure 3 illustrates the results of our preliminary study on the effects on the development of *T. gondii* and *P. falciparum*. In the experiment, which was designed to determine the IC_{50} of compound 1 against *T. gondii* (Fig. 3a), we noticed that the treatment of intracellular tachyzoites led to an overall reduction of parasitophorous vacuoles and a decrease in the number of parasites per vacuole (see also Fig. 3b). The successful development of tachyzoites can be summarized as a series of obligatory steps, i.e., gliding of the parasites, attachment to the host cell, conoid extrusion, active invasion with formation of a tight junction, sequential secretion of proteins from micronemes and rhoptry neck, formation of a parasitophorous vacuole, and reprogramming of the host cell and intravacuolar division by endodyogeny. Compound 1 had no visible effect on gliding capacities based on an *in vitro* motility assay (see Fig. S1 in the supplemental material). Compound 1 did not inhibit the *in vitro* extrusion of the conoid induced by ionomycin (31), and we did not observe any effect on the microneme secretion-induced ethanol (32) (data not shown).

We sought to determine whether the treatment with compound 1 affects the intracellular proliferation of *T. gondii* tachyzoites using direct observation by phase-contrast micros-

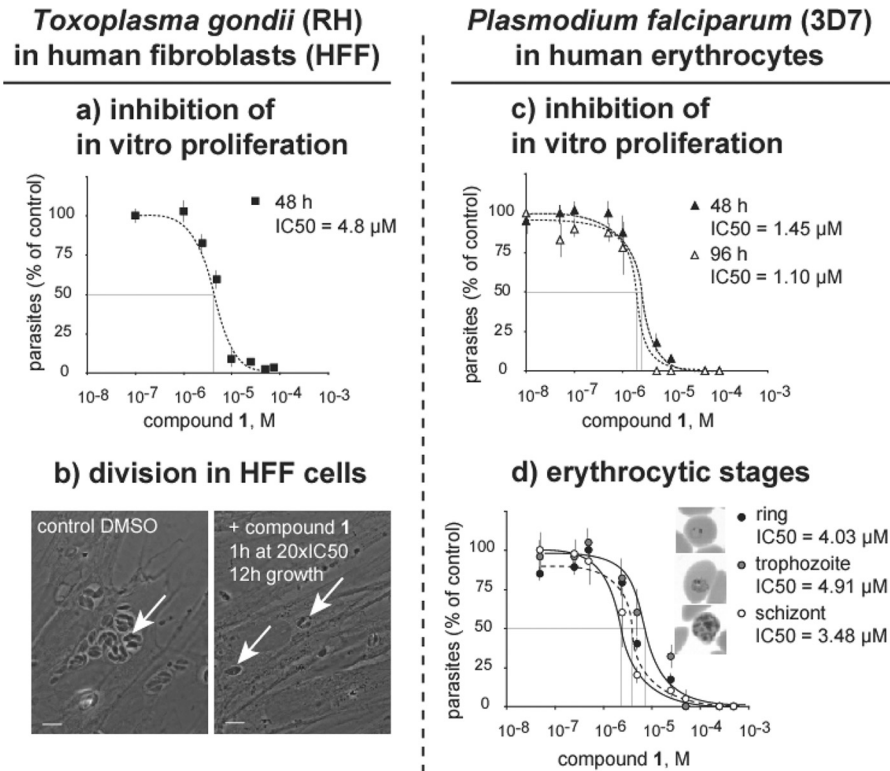


FIG 3 Preliminary analysis of the *in vitro* antiparasitic properties of compound 1, harboring the benzimidazolone-piperidinyl chemotype, on *T. gondii* and *P. falciparum*. Compound 1 was selected for a concise and preliminary analysis of the potential effects of the benzimidazolone-piperidinyl chemotype on *T. gondii* (RH strain) and *P. falciparum* (3D7 strain) at its blood stages, based on an IC_{50} of $<5 \mu\text{M}$ in both models. *T. gondii* was grown in human fibroblasts (HFF cells) and *P. falciparum* in human erythrocytes. (a and b) Effects of compound 1 on *T. gondii*. (a) Effect of compound 1 on proliferation of parasites. IC_{50} s were determined on RH strain grown in HFF cells. The parasites were grown in HFF cells. Parasitophorous vacuoles containing 8 to 32 parasites under control conditions or 1 to 2 parasites after treatment are indicated by white arrows. Scale bar, $1 \mu\text{m}$. (b) Effect on intracellular division of tachyzoites. (c and d) Effect of compound 1 on *P. falciparum*. (c) Effect of compound 1 on proliferation of parasites. IC_{50} s were determined on 3D7 strain grown in red blood cells. IC_{50} s were determined after one (at 48 h [▲]) or two (at 96 h [△]) cell divisions so as to detect any delayed cell death phenotype due to an impairment of the apicoplast. (d) Effect of compound 1 on erythrocytic stages. IC_{50} s were determined in synchronized parasites' culture. Captions illustrate ring, trophozoite, and schizont stages. Scale is given by red blood cell radius, i.e., $7 \mu\text{m}$. IC_{50} s are indicated with dotted lines in the graphs.

copy and parasite numeration. Tachyzoites were treated for 1 h with compound 1 at concentrations ranging from IC_{50} to $20\times IC_{50}$. The parasites were then allowed to invade HFF host cells and were grown for 12 h before observation and cell counting. **Figure 3b** shows that the number of parasites strongly decreased after treatment with compound 1. After 12 h under control conditions, *Toxoplasma* cells reached a number of 8 to 32 parasites per parasitophorous vacuole. In contrast, when parasites were treated for 1 h in the presence of compound 1 prior to HFF infection, the numbers of parasitophorous vacuoles per field and of parasites per vacuole decreased with increasing concentrations of the compound. At $20\times IC_{50}$, corresponding to an absence of proliferation following the colorimetric titration assay, the number of vacuoles was nevertheless 35% of the control, with parasitophorous vacuoles containing only 1 to 2 parasites each (**Fig. 3b**). When compound 1 was supplied after the invasion of HFF cells, similar results were obtained. Based on this initial study, we concluded that the effect of compound 1 was likely attributable to a deleterious effect during the cellular division of *Toxoplasma*.

(ii) ***In vitro* effects of compound 1 on *P. falciparum* blood stages.** We briefly investigated the effect of compound 1 on two features of the erythrocytic life stage of *P. falciparum*. First, we considered that important processes of glycerolipid metabolism

occur in two compartments of the cell, i.e., the ER and the apicoplast (see the introduction). It has been shown that most drugs affecting apicoplast maintenance induced a delayed death phenotype, i.e., one that occurred after two full division cycles (9, 44, 45). In *P. falciparum* blood stages, a delayed death effect can only be observed after two full intraerythrocytic cycles, around 96 h postinfection (46, 47). We analyzed the effect of treatment with increasing doses of compound 1 after 48 h and 96 h of *P. falciparum* 3D7 development and did not detect any significant change (**Fig. 3c**). This result suggests that apicoplast maintenance is not impaired by compound 1.

During the *P. falciparum* blood stage, glycerolipid synthesis is highest during the late stages of development, i.e., the mid-trophozoite and schizont stages, when the biogenesis of daughter cell compartments occurs (48). Since the IC_{50} of the tested piperidinyl-benzimidazolone analog was determined on asynchronous cultures, it was not possible to evaluate the activities on the different intraerythrocytic stages. Thus, we measured the IC_{50} of compound 1 on synchronized ring, trophozoite, and schizont cultures. Compound 1 was similarly active against early stage (ring) and mature stages (trophozoite and schizont) (**Fig. 3d**).

We investigated the effect of compound 1 on various strains of *P. falciparum* that are sensitive (Nigerian and 3D7) or resistant

TABLE 1 Inhibitory properties of compound 1 on various strains of *Plasmodium falciparum*^a

	Average IC ₅₀ (M) of:			
	Chloroquine-sensitive strain:		Chloroquine-resistant strain:	
	Nigerian	3D7	W2	Dd2
Compound 1	1.20 × 10 ⁻⁵	1.45 × 10 ⁻⁶	1.05 × 10 ⁻⁶	1.35 × 10 ⁻⁶
Chloroquine	3.20 × 10 ⁻⁸	1.03 × 10 ⁻⁸	9.90 × 10 ⁻⁸	1.72 × 10 ⁻⁷
Artemisinin	ND ^b	2.87 × 10 ⁻⁸	ND	6.30 × 10 ⁻⁸
Artesunate	ND	9.70 × 10 ⁻⁹	ND	1.16 × 10 ⁻⁸
Triclosan	ND	1.55 × 10 ⁻⁶	ND	2.10 × 10 ⁻⁶

^a Assays were performed using chloroquine-sensitive (Nigerian, 3D7) or resistant (W2, Dd2) strains. The IC₅₀s of other antimalarials (chloroquine, artemisinin, artesunate, and triclosan) were determined in parallel experiments. Each value is the average from two independent experiments.

^b ND, not determined.

(W2 and Dd2) to chloroquine. **Table 1** shows that the IC₅₀ of compound 1 was in the 1 to 10 μM range. In the 3D7 strain, we compared the IC₅₀ of compound 1 with that of antimalarials known to be active *in vitro* and *in vivo*, i.e., chloroquine, artemisinin, and artesunate (all with IC₅₀s in the 10 nM range in our *in vitro* system) (**Table 1**) and triclosan, which is known to be efficient only *in vitro* (in the micromolar range) (**Table 1**).

(iii) *In vitro* cytotoxicity of compound 1 on human cell models and determination of an *in vitro* selectivity index. Since targets of piperidinyl-benzimidazolones may be shared between the parasites and their human host cells, pharmacological activity might be totally or partly due to a nonspecific cytotoxic effect. Before exploring a library of piperidinyl-benzimidazolone analogs, we analyzed the inhibitory properties of compound 1 on various proliferating human cell models. As an initial investigation, we assessed the effect of piperidinyl-benzimidazolones on the morphology and the proliferation of *T. gondii* host cells, i.e., confluent or proliferative HFF cells (not shown). A 12-h treatment with high concentration of compound 1 (100 μM) had no effect on the cytoskeleton integrity of HFF, as observed by light microscopy and immunofluorescence assays (using microtubule, actin, and focal adhesion point probes, i.e., anti-tubulin antibodies, phalloidin, and anti-vinculin antibodies, respectively; not shown). Similarly, compound 1 did not have any effect on the division of growing HFF cells when treated at 50 or 100 μM for 24 h. We then set up a protocol to address the cytotoxicity of compound 1 on more versatile/sensitive human cells. **Table 2** shows that compound 1 inhibited the growth of erythroblast (K-562) and monocyte (THP-1) cell lines with IC₅₀s ranging from 15 to 20 μM and the growth of both lymphoblast (Jurkat) and macrophage (U-937) cell lines with IC₅₀s of >170 μM. There is therefore >1 log between the effect on parasites and that on human cells, indicating a relative selectivity of compound 1.

Taking K-562 cells as a standard model for comparison, we calculated a selectivity index (SI), defined as the IC₅₀ value determined on a human cell model (cytotoxicity) divided by the IC₅₀ value determined on parasites. **Table 3** shows that using this standard cell model, we determined an SI for compound 1 of 13.72 on *P. falciparum* and 3.43 on *T. gondii*.

Two-step exploration of the library of piperidinyl-benzimidazolone analogs. The exploration of the library was performed in two steps, so as to select compounds with lower IC₅₀s against *T.*

TABLE 2 Inhibitory properties of compound 1 on the *in vitro* proliferation of various human cell models^a

Antimalarial	Average IC ₅₀ (M) for:			
	Jurkat	K-562	THP-1	U-937
Compound 1	1.74 × 10 ⁻⁴	1.99 × 10 ⁻⁵	1.48 × 10 ⁻⁵	2.62 × 10 ⁻⁴
Chloroquine	ND ^b	1.10 × 10 ⁻⁵	ND	ND
Artemisinin	ND	1.00 × 10 ⁻⁴	ND	ND
Artesunate	ND	1.06 × 10 ⁻⁶	ND	ND
Triclosan	ND	1.34 × 10 ⁻⁵	ND	ND

^a Lymphoblasts (Jurkat), erythroblasts (K-562), monocytes (THP-1), and macrophages (U-937) were subjected to various concentrations of compound 1 in order to determine the IC₅₀ of toxicity based on cell proliferation. The IC₅₀s of other antimalarials (chloroquine, artemisinin, artesunate, and triclosan) were determined in parallel experiments. Each value is the average from two independent experiments.

^b ND, not determined.

gondii or *P. falciparum* and improved SIs. In the first step, we analyzed the effects of the 250 compounds on the *in vitro* proliferation of both parasites and determined the corresponding IC₅₀s (see Table S1 in the supplemental material). We selected the 114 compounds having an *in vitro* antiparasitic effect with an IC₅₀ of ≤2 μM for at least one parasitic model. **Figure 4a** shows that some compounds (i) had more powerful effects against *T. gondii*, with IC₅₀s in the 100 to 200 nM range (e.g., compounds 4 and 7), (ii) had more potent effects against *P. falciparum*, also in the 100 to 200 nM range (e.g., compounds 8 and 12), and (iii) eventually were equally efficient against both parasites (e.g., compound 13). We did not detect any strong correlation between the IC₅₀ values measured on *T. gondii* and *P. falciparum*.

In the second step, we determined the *in vitro* toxicities of the 114 selected compounds on human K-562 erythroblasts (see Table S2 in the supplemental material). The IC_{50K-562} values allowed us to calculate SIs. **Figure 4b** shows a plot of the SIs determined for each compound on *Toxoplasma* and *Plasmodium*. The compounds with the lowest values have higher adverse effects in this standard assay, and the compounds with the highest values are likely to be selective to the parasites. The chemical library we explored allowed for the identification of compounds with better properties than the initial compound 1. Compounds 4 and 7 acted more specifically against *T. gondii*, compounds 8 and 12 acted more specifically against *P. falciparum*, and compound 13 acted on both parasites; these also displayed improved SIs (**Fig. 4b**).

Remarkably, the SIs of compounds 4 and 7 for *T. gondii* (versus mammalian cells) were 488 and 275, respectively (**Table 3**). These values are promising for the development of antitoxoplasmic drug candidates. The SI values of compounds 8 and 12 relative to *P. falciparum* were 1,078 and 74, close to the SI values obtained with chloroquine or artesunate (1,068 and 109, respectively), which were measured in parallel using our assay, and were lower than that of artemisinin, i.e., 3,484 (**Table 3**). Additionally, the SIs of these compounds were determined against human hepatocellular carcinoma cells (HepG2), providing information regarding the hepatotoxicity of these compounds (**Table 3**). The SIs of compounds 8 and 12 are both >100, as expected for antimalarial lead compounds, tested here in parallel under similar conditions (IC_{50HepG2} 84 and >460 μM for compounds 12 and 8, respectively), with compound 8 showing a selectivity of >2,000. The treatment of *P. falciparum* parasites with compounds 8 and 12 affected parasite proliferation within the first growth cycle (first 24 h), similar to that observed for compound 1. The inhibition of

TABLE 3 *In vitro* selectivity indexes of compound 1 and candidate molecules 4 and 7 identified in this work^a

	<i>In vitro</i> antimalarial activity			<i>In vitro</i> antitoxoplasmic activity	
	IC ₅₀ (3D7) (M)	SI [IC ₅₀ (K-562)/IC ₅₀ (3D7)]	SI [IC ₅₀ (HepG2)/IC ₅₀ (3D7)]	IC ₅₀ (RH) (M)	SI [IC ₅₀ (K-562)/IC ₅₀ (RH)]
Compound 1	1.45 × 10 ⁻⁶	13.72	ND ^b	4.80 × 10 ⁻⁶	3.43
Chloroquine	1.03 × 10 ⁻⁸	1,068	ND		
Artemisinin	2.87 × 10 ⁻⁸	3,484	ND		
Artesunate	9.70 × 10 ⁻⁹	109	ND		
Triclosan	1.55 × 10 ⁻⁶	8.65	ND	3.20 × 10 ⁻⁷	41.87
Compound 8	2.30 × 10 ⁻⁷	1,078	>2,000		
Compound 12	1.80 × 10 ⁻⁷	74	469		
Compound 4				1.81 × 10 ⁻⁷	488
Compound 7				2.00 × 10 ⁻⁷	275

^a The selectivity index (SI) is defined as the ratio of the IC₅₀ value determined on a human cell model (cytotoxicity) to the IC₅₀ value determined on *P. falciparum* (antiplasmodial activity) or *Toxoplasma gondii*. K-562 erythroblasts, HepG2 human hepatocellular carcinoma cells, *P. falciparum* 3D7, and *T. gondii* RH strains were selected as standards for comparison. The SIs of other antimalarials were also determined.

^b ND, not determined.

Plasmodium by compound 12, supplied at a 2 × IC₅₀, was irreversible after a 12-h incubation (not shown). Taken together, these data show that the exploration of the chemical space of piperidinyl-benzimidazolone analogs led to the identification of compounds with *in vitro* properties comparable to those of validated antiparasitic molecules currently used in therapeutic treatments, although their *in vivo* efficacy still needs to be improved.

Interactions of compounds 8 and 12 with artemisinin in *in vitro* trials against *P. falciparum*. We used isobolograms to evaluate the *in vitro* interaction of two of the compounds acting against *P. falciparum*, i.e., compounds 8 and 12, with the front-line antimalarial artemisinin. To that end, *P. falciparum* was incubated with compound-artemisinin combinations described in Materials and Methods. Concentrations of each compound were expressed as fractional inhibitory concentrations (FIC), i.e., the fraction of the IC₅₀s of compounds when tested alone. The isobolograms in Fig. 5 show that interaction of compounds 8 and 12 with artemisinin were similar: under all conditions, the summed FIC (ΣFIC) measured for each compound-artemisinin combination was close to 1.0 or slightly higher. None of the ΣFICs were >2.0, which is regarded as a cutoff for antagonism (37–39). These results indicate that the interaction between compound 8 or 12 and artemisinin is additive.

Analysis of the structure-activity relationship of compounds with *in vitro* antiproliferating activity against *T. gondii* and *P. falciparum*. Figure 6 summarizes the structure-activity relationship (SAR) trends that can be deduced from the chemical structures of compounds, their *in vitro* pharmacological activities against *T. gondii* or *P. falciparum*, and their low *in vitro* adverse effects on human K-562 cells. Here, we propose two distinct SAR models, one for each of the tested *Apicomplexa* parasites, which have shared but also diverging features.

Considering parts A and B, only a few changes could be made that would lead to beneficial effects. Part A was modulated with a complete substitution of the benzimidazolone by a 1-phenyl-1,3,8-triazaspiro[4,5]decan-4-one scaffold (a substructure found in VU0285655, a specific inhibitor of PLD2) and still exhibited antitoxoplasmic properties (Fig. 6a). In contrast, its antimalarial property was improved when part A was substituted with phenylsulfonamide or phenylbenzenesulfonamide (Fig. 6b). At the level of part B, although the piperidine cycle was essential for the effects against *Plasmodium*, some modifications could be made without

decreasing the antitoxoplasmic properties, as long as only one N atom was present and no double bonds were added (Fig. 6b). Parts A and B are critical for the molecular mode of action of galvestine-1 and halopemide at the level of their respective enzymatic targets. The importance of the structural motifs in parts A and B in the antiparasitic activities is therefore consistent with interference with a glycerolipid-manipulating system.

Part C was important in both *T. gondii* and *P. falciparum*, leading to a complete loss of antiparasitic activity when absent from the piperidinyl-benzimidazolone scaffold. Aromatic cycles were beneficial over different hydrophobic groups, like alkyl chains. When considering the effects on *Plasmodium*, the dibenzylamido ethoxy group appeared to be essential (Fig. 6b), whereas modulations were possible relative to the effects against *Toxoplasma*. This difference suggests that selectivity on *P. falciparum* is partly due to the dibenzylamido ethoxy motif, which was not initially thought to interfere with glycerolipid-manipulating enzymes (40), and this feature suggests that off- or promiscuous target(s) might be responsible for part of the effect on the malaria parasite. Compounds with a part C similar to that of VU0285655 were efficient against *Plasmodium* in spite of the absence of a PLD2, indicating that the dibenzylamido ethoxy group might be avoided to limit possible effects on undesired targets.

Therefore, the SAR analyses indicate that compounds with improved efficacies after changes in parts A and B are consistent with changes in selectivity on targets possibly acting in glycerolipid metabolism, and that SAR in part C should be refined, especially relative to the antimalarial activity.

DISCUSSION

Previous analyses of piperidinyl-benzimidazolone analogs have shown that this chemotype is a novel source for identifying compounds acting specifically on enzymes manipulating DAG (like plant MGD enzymes) (23, 40) or PC/PA (like human PLDs) (41, 42) (Fig. 1). The mode of action of these compounds involves their binding at the level of the substrate-binding and/or catalytic sites, and at least in one case, it was shown that inhibition was due to competition with the binding of the DAG structure (23). The two-dimensional chemical structure of the piperidinyl-benzimidazolone chemotype has no obvious similarity with the DAG-PA structure (see Fig. 1); nevertheless, three-dimensional modeling of galvestine-1 and DAG has shown that part of the structures of

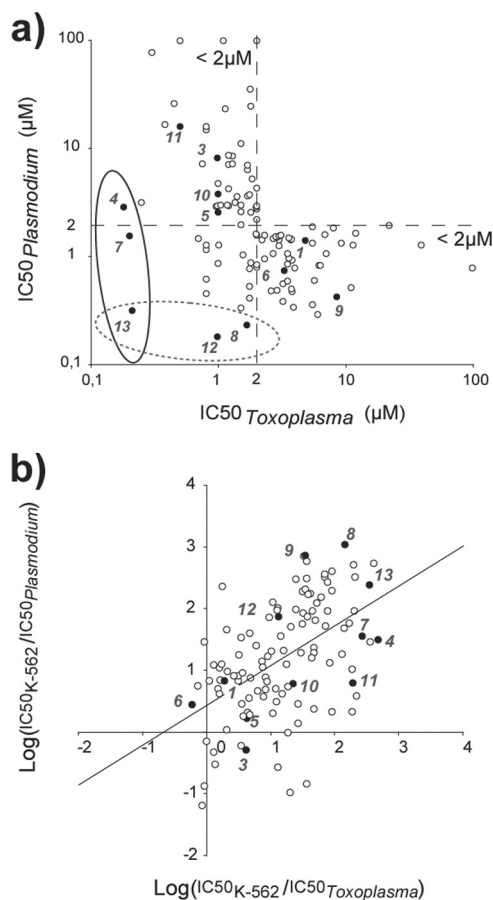


FIG 4 Two-step exploration of the library of piperidinyl-benzimidazolone analogs. (a) Step 1: selection of compounds inhibiting *T. gondii* or *P. falciparum* *in vitro* proliferation with an IC_{50} of $\leq 2 \mu M$. The effects of all 250 compounds on the *in vitro* proliferation of both parasites were determined via IC_{50} measurement. The corresponding IC_{50} s (see Table S1 in the supplemental material) were used to select 114 compounds having an *in vitro* antiparasitic efficacy with an IC_{50} of $\leq 2 \mu M$ on at least one parasitic model to perform subsequent analyses. The graph highlights compounds acting with the lowest IC_{50} s against *T. gondii* (circled in solid line) or *P. falciparum* (circled in dotted line). (b) Step 2, analyses of the selectivity indexes. The selectivity index (SI) is defined as the ratio of the IC_{50} value determined on a human cell model (cytotoxicity) to the IC_{50} value determined on *P. falciparum* or *T. gondii*. We selected K-562 erythroblasts, *P. falciparum* 3D7, and *T. gondii* RH strains as standards for comparisons. The numbers and respective closed circles correspond to the compounds illustrated in Fig. 2.

the inhibitors might superimpose the glycerol moiety of the DAG structure, using superimposed H-bond acceptors (23).

In *Apicomplexa*, neither the target for galvestine-1 (MGDG synthases or MGDs) nor that of halopemide and VU0285655 (PLDs) has been identified. No genes coding for MGDs or PLDs were identified in the genomes of the parasites. Considering MGDs, the incorporation of radiolabeled galactose from UDP-galactose into a lipid having chromatographic properties similar to those of MGDG has been reported in *T. gondii*- and *P. falciparum*-permeabilized cells (49) but was not detected in *P. falciparum* microsomes (50). The actual presence of MGDG in these parasites was not detected by sensitive mass spectrometry (15, 51). In the absence of any clear homolog gene, it is thus likely that plastid MGDG synthases have been lost or have strongly diverged in the course of the *Apicomplexa* evolution. Considering PLDs, the ap-

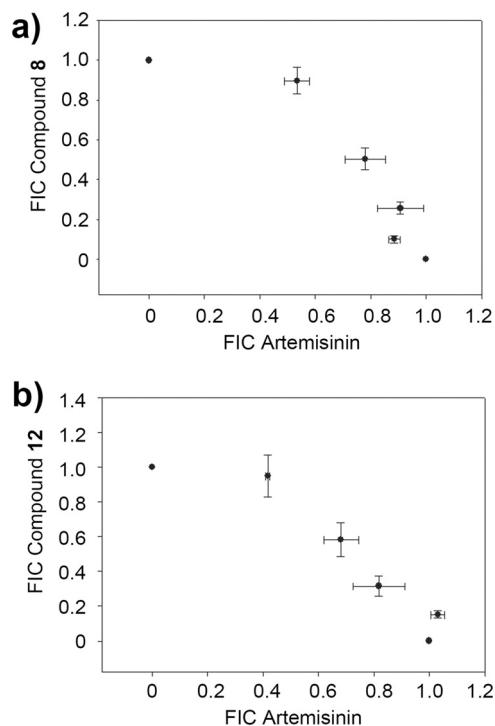


FIG 5 Isobolograms showing the antimalarial additivity between compounds 8 (a) or 12 (b) and artemisinin. The compound concentrations are expressed as the fractional inhibitory concentration (FIC). For each compound-artemisinin combination, ΣFIC values need to be < 0.5 or > 2 to represent synergism or antagonism, respectively (see Materials and Methods). Both isobolograms indicate neutral interactions. The data are averaged from 3 independent experiments, each carried out in triplicate. The error bars represent the standard error of the mean (SEM).

parent lack of this phospholipase class is puzzling, since this enzyme might be a tool for diverting and scavenging glycerolipids from the host cell. Other protein candidates, among which PA-synthesizing acyltransferases, PAPS, DGKs, PLCs, phospholipase A2s (PLA2s), and virtually all enzymes synthesizing phospholipid classes might manipulate DAG-PA structures in *Apicomplexa* cells. In addition, since DAG, PA, and some phospholipids are not only metabolites but also secondary messengers, possible targets include DAG- and PA-activated proteins.

The library of compounds we explored contains all the structural motifs that have proven to be essential for driving galvestine-1, halopemide, and VU0285655 specificity, including the 1-phenyl-1,3,8-triazaspiro[4,5]decan-4-one scaffold and intense changes at the level of piperidinyl-benzimidazolone moiety (Fig. 2). Since the rationale for this study was to attempt to interfere with a process occurring in the core of biomembranes, the presence of a hydrophobic part (part C) to promote a partitioning of the compounds inside the membrane phase was also investigated by substitution with other cyclic structures and alkyl chains.

Our preliminary analysis of the effects of compound 1 on parasite and human cell models has shown that this compound acts on both parasites (*T. gondii* and *P. falciparum*), with IC_{50} s in the 1 to 10 μM range. In *T. gondii*, compound 1 interfered specifically with cell division. This first set of results (Fig. 3a and b) supports that compound 1 acts on parasite multiplication, which is expected if membrane biogenesis was targeted. In *Plasmodium*, compound 1 inhibited the proliferation of parasites in red blood

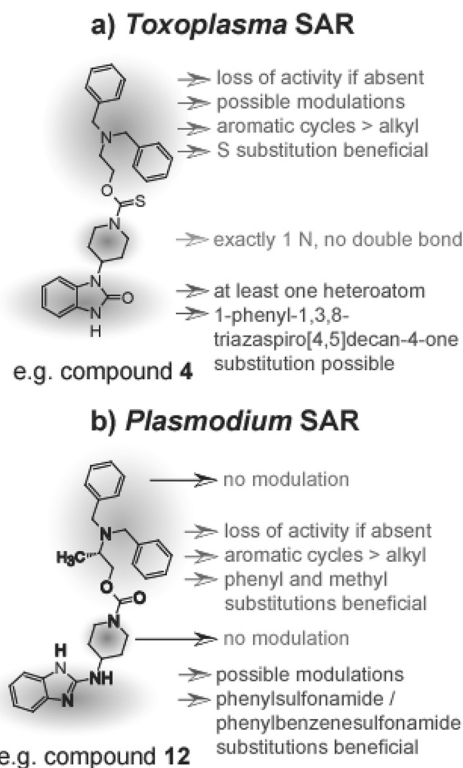


FIG 6 Structure-activity relationship (SAR) analysis of compounds acting more specifically on *T. gondii* and on *P. falciparum*. SAR trends were deduced from the activities of compounds on the *in vitro* proliferation of parasites and on human cells, including IC_{50} and SI values. (a) SAR model correlating the structure of tested compounds with the efficacy on *T. gondii*. SAR trends are illustrated using the structure of compound 4. (b) SAR model correlating the structure of tested compounds with the efficacy on *P. falciparum*. SAR trends are illustrated using the structure of compound 12. No modulation, changes of the group lead to a partial or total loss of biological activity.

cells regardless of the erythrocytic stage (Fig. 3c and d). The effect of compound 1 was incompatible with a delayed death phenotype and thus seemed to rule out an impairment of apicoplast maintenance (Fig. 3c and d). Piperidiny-benzimidazolones might act on lipid metabolism occurring in another compartment, with the ER being a likely target. The synthesis of analogs associated with a fluorescent probe and localization study may reveal the site of action of piperidiny-benzimidazolones.

Compound 1 showed an efficacy on all tested strains of chloroquine-sensitive and chloroquine-resistant strains of *P. falciparum* (Table 1). The *in vitro* toxic effects in human cells were determined to be in the 15 to 200 μ M range (Table 2). Using K-562 human erythrocytes as a standard, we estimated a selectivity index (SI) for subsequent comparisons of the compounds (Table 3).

We explored the 250-compound library of piperidiny-benzimidazolone analogs in two steps. After selection of 114 compounds with IC_{50} s of ≤ 2 μ M against at least one of the tested parasites (Fig. 4a), we determined the effects on K-562 cells, allowing for comparisons of the SIs (Fig. 4b). A weak linear correlation was detected between the SIs determined relative to each parasite (Fig. 4b) (linear correlation: $y = 0.6429x + 0.4342$; $R^2 = 0.256$). This indicates that a structural correlation exists in compounds acting on both *Apicomplexa* models but that species-specific structures likely exist. Indeed, compounds 4 and 7 appear to be more

specific against *T. gondii*, while compounds 8 and 12 are more efficient against *P. falciparum* (Fig. 4a). When tested on the *in vitro* proliferation of *Eimeria tenella* infecting bovine MDBK cells, we did not detect any antiparasitic effect of compound 8 < 100 μ M. Compound 12 had *in vitro* inhibitory effects on *Eimeria*, with an IC_{50} in the 1 to 2 μ M range and no cytotoxicity on Madin-Darby bovine kidney (MDBK) cells at these concentrations (not shown). These results support species-specific properties within the *Apicomplexa* phylum. This study also highlighted compounds with an improved SI compared to that of compound 1, with SIs of 488 for compound 4 and 275 for compound 7 against *T. gondii*, and SIs of 1,078 for compound 8 and 74 for compound 12 against *P. falciparum*. These SIs are in the range of those measured for the other drugs we tested in parallel, such as chloroquine (SI, 1,068) or artesunate (SI, 109) (Table 3).

As part of our strategy to develop new molecules for therapeutic intervention, we assessed the toxicities of the two best compounds, 8 and 12, acting against *Plasmodium*. BALB/c mice received four daily injections at 50 mg \cdot kg of body weight⁻¹. No toxic effect was observed after ≥ 20 days after the first injection (not shown), correlating with the low *in vitro* toxicities of these molecules. A similar experiment was conducted on BALB/c mice infected by *Plasmodium vinckei* and treated at 25 mg \cdot kg⁻¹ in a 4-day injection trial (52, 53). Parasitemia following treatment with compound 12 was significantly reduced on days 3 and 4 (see Fig. S2 in the supplemental material). However, no curative effect was observed. This assay suggests that compound 12 limits the proliferation of parasites *in vivo* and delays parasitemia, but the molecule properties should be further optimized to reach a complete cure. Such limited *in vivo* activities are not uncommon for a trial based on the initial formulation of a candidate drug. They should guide the design of new analogs with antimalarial activity based on the compound 12 scaffold. Isobole analyses of the interaction of compounds 8 and 12 with artemisinin (Fig. 5) indicate that the interaction is additive. It is thus possible to explore the potential benefits of these compounds in artemisinin-based combination therapies (ACTs).

We performed a preliminary proteomic analysis in order to identify possible target proteins in *P. falciparum* (described in the supplemental material). We based our analysis on a piperidiny-benzimidazolone analog, which is linked to biotin. We grafted this analog to a NeutrAvidin matrix and chromatographed red blood cells (mock) or *P. falciparum* protein extracts, focusing on soluble and insoluble proteins in parallel experiments. We then analyzed the proteomic profiles of the proteins bound to the affinity matrix by mass spectrometry. In the mock (red blood cell) trials, we detected only a very low level of hemoglobin contaminant together with avidin released from the affinity matrix. In the *P. falciparum* extract, we detected 12 major polypeptides, including a protein acting on an acyl-containing substrate (a substructure also found in diacylglycerol and phosphatidic acid), a pyruvate kinase (acting in the pyruvate hub upstream of fatty acid synthesis), an enzyme manipulating glycerone-P and glyceraldehyde-3-P, which are close to the glycerol backbones of diacylglycerol and phosphatidic acid. We also detected proteins of unknown function. Based on these experiments, we obtained a list of putative proteins binding the biotinylated compound, which should be characterized in greater detail in the future to check if they are also inhibited and if the genetic impairment is lethal. Additional proteins eluted from

the affinity matrix have been detected in smaller amounts and shall be also analyzed.

Taken together, *in vitro* and *in vivo* trials reported in this article indicate that we refined compound structures, which consistently had a possible effect on membrane glycerolipids, and that we gained in *in vitro* efficacy reaching the range of the antiparasitic drugs tested in parallel. In-depth analyses of the biological response of parasites should be undertaken to provide clues on the cellular modes of action of these novel drugs. More improvements should be made to develop molecules acting *in vivo* in mono- or multitherapies. Future developments should therefore benefit from the SAR models we proposed here.

ACKNOWLEDGMENTS

This work was supported by Oséo-Anvar, Conseil Régional Rhône-Alpes (PhD grant allocated to N.S.), Agence Nationale de la Recherche (Plasmo-Explore, PlasmoExpress, ReGal, and DiaDomOil grants allocated to E.M.), the European Commission (FP7 OIF Marie Curie Fellowship, project Apicolipid, allocated to C.Y.B.), Labex GRAL (to E.M.), and a joint program of the French Ministry of Foreign Affairs and the South African Department of Sciences and Technologies (E.M. and L.-M.B.).

We thank Ricardo Mondragon for advice on gliding assays, Lauriane Kuhn and the EDyP laboratory for proteomic analyses presented in the supplemental material, and Christian Vincent and Dean Goodman for fruitful discussions.

REFERENCES

- Morrison DA. 2009. Evolution of the *Apicomplexa*: where are we now? *Trends Parasitol.* 25:375–382. <http://dx.doi.org/10.1016/j.pt.2009.05.010>.
- WHO. 2011. World malaria report: 2011. World Health Organization, Geneva, Switzerland. <http://www.who.int/malaria/publications/atoz/9789241564403/en/>.
- Sukthana Y. 2006. Toxoplasmosis: beyond animals to humans. *Trends Parasitol.* 22:137–142. <http://dx.doi.org/10.1016/j.pt.2006.01.007>.
- Limenitakis J, Soldati-Favre D. 2011. Functional genetics in *Apicomplexa*: potentials and limits. *FEBS Lett.* 585:1579–1588. <http://dx.doi.org/10.1016/j.febslet.2011.05.002>.
- Tarun AS, Vaughan AM, Kappe SH. 2009. Redefining the role of *de novo* fatty acid synthesis in *Plasmodium* parasites. *Trends Parasitol.* 25:545–550. <http://dx.doi.org/10.1016/j.pt.2009.09.002>.
- Dechamps S, Shastri S, Wengelnik K, Vial HJ. 2010. Glycerophospholipid acquisition in *Plasmodium*—a puzzling assembly of biosynthetic pathways. *Int. J. Parasitol.* 40:1347–1365. <http://dx.doi.org/10.1016/j.ijpara.2010.05.008>.
- Mi-Ichi F, Kita K, Mitamura T. 2006. Intraerythrocytic *Plasmodium falciparum* utilize a broad range of serum-derived fatty acids with limited modification for their growth. *Parasitology* 133:399–410. <http://dx.doi.org/10.1017/S0031182006000540>.
- Mazumdar J, Striepen B. 2007. Make it or take it: fatty acid metabolism of apicomplexan parasites. *Eukaryot. Cell* 6:1727–1735. <http://dx.doi.org/10.1128/EC.00255-07>.
- Botté CY, Dubar F, McFadden GI, Maréchal E, Biot C. 2012. *Plasmodium falciparum* apicoplast drugs: targets or off-targets? *Chem. Rev.* 112:1269–1283. <http://dx.doi.org/10.1021/cr200258w>.
- Santiago TC, Zufferey R, Mehra RS, Coleman RA, Mamoun CB. 2004. The *Plasmodium falciparum* PfGatp is an endoplasmic reticulum membrane protein important for the initial step of malarial glycerolipid synthesis. *J. Biol. Chem.* 279:9222–9232. <http://dx.doi.org/10.1074/jbc.M310502200>.
- Dubots E, Botté C, Boudière L, Yamaro-Botté Y, Jouhet J, Maréchal E, Block MA. 2012. Role of phosphatidic acid in plant galactolipid synthesis. *Biochimie* 94:86–93. <http://dx.doi.org/10.1016/j.biochi.2011.03.012>.
- Raabe A, Berry L, Sollelis L, Cerdan R, Tawk L, Vial HJ, Billker O, Wengelnik K. 2011. Genetic and transcriptional analysis of phosphoinositide-specific phospholipase C in *Plasmodium*. *Exp. Parasitol.* 129:75–80. <http://dx.doi.org/10.1016/j.exppara.2011.05.023>.
- Fang JM, Marchesini N, Moreno SNJ. 2006. A *Toxoplasma gondii* phosphoinositide phospholipase C (TgPI-PLC) with high affinity for phosphatidylinositol. *Biochem. J.* 394:417–425. <http://dx.doi.org/10.1042/BJ20051393>.
- Botté CY, Yamaro-Botté Y, Janouskovec J, Rupasinghe T, Keeling PJ, Crellin P, Coppel RL, Maréchal E, McConville MJ, McFadden GI. 2011. Identification of plant-like galactolipids in *Chromera velia*, a photosynthetic relative of malaria parasites. *J. Biol. Chem.* 286:29893–29903. <http://dx.doi.org/10.1074/jbc.M111.254979>.
- Botté C, Saidani N, Mondragon R, Mondragón M, Isaac G, Mui E, McLeod R, Dubremetz JF, Vial H, Welti R, Cesbron-Delauw MF, Mercier C, Maréchal E. 2008. Subcellular localization and dynamics of a digalactolipid-like epitope in *Toxoplasma gondii*. *J. Lipid Res.* 49:746–762. <http://dx.doi.org/10.1194/jlr.M700476-JLR200>.
- Botté CY, Yamaro-Botté Y, Rupasinghe TW, Mullin KA, MacRae JI, Spurck TP, Kalanon M, Shears MJ, Coppel RL, Crellin PK, Maréchal E, McConville MJ, McFadden GI. 2013. Atypical lipid composition in the purified relict plastid (apicoplast) of malaria parasites. *Proc. Natl. Acad. Sci. U. S. A.* 110:7506–7511. <http://dx.doi.org/10.1073/pnas.1301251110>.
- MacRae JI, Maréchal E, Biot C, Botté CY. 2012. The apicoplast: a key target to cure malaria. *Curr. Pharm. Des.* 18:3490–3504. <http://dx.doi.org/10.2174/138161212801327275>.
- Min Y, Kumar TRS, Nkrumah LJ, Coppi A, Retzlaff S, Li CD, Kelly BJ, Moura PA, Lakshmanan V, Freundlich JS, Valderramos JC, Vilcheze C, Siedner M, Tsai JHC, Falkard B, Sidhu AB, Purcell LA, Grattraud P, Kremer L, Waters AP, Schiehser G, Jacobus DP, Janse CJ, Ager A, Jacobs WR, Jr, Sacchetti JC, Heussler V, Sinni P, Fidock DA. 2008. The fatty acid biosynthesis enzyme FabI plays a key role in the development of liver-stage malarial parasites. *Cell Host Microbe* 4:567–578. <http://dx.doi.org/10.1016/j.chom.2008.11.001>.
- Vaughan AM, O'Neill MT, Tarun AS, Camargo N, Phuong TM, Aly AS, Cowman AF, Kappe SH. 2009. Type II fatty acid synthesis is essential only for malaria parasite late liver stage development. *Cell. Microbiol.* 11:506–520. <http://dx.doi.org/10.1111/j.1462-5822.2008.01270.x>.
- Wengelnik K, Vidal V, Ancelin ML, Cathiard AM, Morgat JL, Kocken CH, Calas M, Herrera S, Thomas AW, Vial HJ. 2002. A class of potent antimalarials and their specific accumulation in infected erythrocytes. *Science* 295:1311–1314. <http://dx.doi.org/10.1126/science.1067236>.
- Caldarelli SA, Hamel M, Duckert JF, Ouattara M, Calas M, Maynadier M, Wein S, Périgaud C, Pellet A, Vial HJ, Peyrottes S. 2012. Disulfide prodrugs of albitalozolium (T3/SAR97276): synthesis and biological activities. *J. Med. Chem.* 55:4619–4628. <http://dx.doi.org/10.1021/jm3000328>.
- González-Bulnes P, Bobenchik AM, Augagneur Y, Cerdan R, Vial HJ, Llebaria A, Ben Mamoun C. 2011. PG12, a phospholipid analog with potent antimalarial activity, inhibits *Plasmodium falciparum* CTP: phosphocholine cytidylyltransferase activity. *J. Biol. Chem.* 286:28940–28947. <http://dx.doi.org/10.1074/jbc.M111.268946>.
- Botté CY, Deligny M, Rocca A, Bonneau AL, Saidani N, Hardré H, Aci S, Yamaro-Botté Y, Jouhet J, Dubots E, Loizeau K, Bastien O, Bréhélin L, Joyard J, Cintrat JC, Falconet D, Block MA, Rousseau B, Lopez R, Maréchal E. 2011. Chemical inhibitors of monogalactosyldiacylglycerol syntheses in *Arabidopsis thaliana*. *Nat. Chem. Biol.* 7:834–842. <http://dx.doi.org/10.1038/nchembio.658>.
- Morisaki JH, Heuser JE, Sibley LD. 1995. Invasion of *Toxoplasma gondii* occurs by active penetration of the host cell. *J. Cell Sci.* 108(Pt 6):2457–2464.
- McFadden DC, Seeber F, Boothroyd JC. 1997. Use of *Toxoplasma gondii* expressing beta-galactosidase for colorimetric assessment of drug activity *in vitro*. *Antimicrob. Agents Chemother.* 41:1849–1853.
- Seeber F, Boothroyd JC. 1996. *Escherichia coli* beta-galactosidase as an *in vitro* and *in vivo* reporter enzyme and stable transfection marker in the intracellular protozoan parasite *Toxoplasma gondii*. *Gene* 169:39–45. [http://dx.doi.org/10.1016/0378-1119\(95\)00786-5](http://dx.doi.org/10.1016/0378-1119(95)00786-5).
- Conseil V, Soëte M, Dubremetz JF. 1999. Serine protease inhibitors block invasion of host cells by *Toxoplasma gondii*. *Antimicrob. Agents Chemother.* 43:1358–1361.
- Håkansson S, Morisaki H, Heuser J, Sibley LD. 1999. Time-lapse video microscopy of gliding motility in *Toxoplasma gondii* reveals a novel, biphasic mechanism of cell locomotion. *Mol. Biol. Cell* 10:3539–3547. <http://dx.doi.org/10.1091/mbc.10.11.3539>.
- Rodríguez C, Afchain D, Capron A, Dissous C, Santoro F. 1985. Major surface protein of *Toxoplasma gondii* (p30) contains an immunodominant region with repetitive epitopes. *Eur. J. Immunol.* 15:747–749. <http://dx.doi.org/10.1002/eji.1830150721>.
- Darcy F, Maes P, Gras-Masse H, Aurialt C, Bossus M, Deslee D,

- Godard I, Cesbron MF, Tartar A, Capron A. 1992. Protection of mice and nude rats against toxoplasmosis by a multiple antigenic peptide construction derived from *Toxoplasma gondii* P30 antigen. *J. Immunol.* **149**: 3636–3641.
31. Mondragon R, Frixione E. 1996. Ca(2+)-dependence of conoid extrusion in *Toxoplasma gondii* tachyzoites. *J. Eukaryot. Microbiol.* **43**:120–127. <http://dx.doi.org/10.1111/j.1550-7408.1996.tb04491.x>.
32. Carruthers VB, Moreno SN, Sibley LD. 1999. Ethanol and acetaldehyde elevate intracellular [Ca²⁺] and stimulate microneme discharge in *Toxoplasma gondii*. *Biochem. J.* **342**(Pt 2):379–386.
33. Charif H, Darcy F, Torpier G, Cesbron-Delauw MF, Capron A. 1990. *Toxoplasma gondii*: characterization and localization of antigens secreted from tachyzoites. *Exp. Parasitol.* **71**:114–124. [http://dx.doi.org/10.1016/0014-4894\(90\)90014-4](http://dx.doi.org/10.1016/0014-4894(90)90014-4).
34. Trager W, Jensen JB. 1976. Human malaria parasites in continuous culture. *Science* **193**:673–675. <http://dx.doi.org/10.1126/science.781840>.
35. Desjardins RE, Pamplin CL, III, von Bredow J, Barry KG, Canfield CJ. 1979. Kinetics of a new antimalarial, mefloquine. *Clin. Pharmacol. Ther.* **26**:372–379.
36. van Schalkwyk DA, Priebe W, Saliba KJ. 2008. The inhibitory effect of 2-halo derivatives of D-glucose on glycolysis and on the proliferation of the human malaria parasite *Plasmodium falciparum*. *J. Pharmacol. Exp. Ther.* **327**:511–517. <http://dx.doi.org/10.1124/jpet.108.141929>.
37. Bell A. 2005. Antimalarial drug synergism and antagonism: mechanistic and clinical significance. *FEMS Microbiol. Lett.* **253**:171–184. <http://dx.doi.org/10.1016/j.femsle.2005.09.035>.
38. Odds FC. 2003. Synergy, antagonism, and what the checkerboard puts between them. *J. Antimicrob. Chemother.* **52**:1. <http://dx.doi.org/10.1093/jac/dkg301>.
39. Johnson MD, MacDougall C, Ostrosky-Zeichner L, Perfect JR, Rex JH. 2004. Combination antifungal therapy. *Antimicrob. Agents Chemother.* **48**:693–715. <http://dx.doi.org/10.1128/AAC.48.3.693-715.2004>.
40. Boudière L, Botté C, Saidani N, Lajoie M, Marion J, Bréhélin L, Yamaro-Botté Y, Satiat-Jeunemaitre B, Breton C, Girard-Egrot A, Bastien O, Jouhet J, Falconet D, Block MA, Maréchal E. 2012. Galvestine-1, a novel chemical probe for the study of the glycerolipid homeostasis system in plant cells. *Mol. Biosyst.* <http://dx.doi.org/10.1039/c2mb25067e>.
41. Monovich L, Mugrage B, Quadros E, Toscano K, Tommasi R, LaVoie S, Liu E, Du Z, LaSala D, Boyar W, Steed P. 2007. Optimization of halopemide for phospholipase D2 inhibition. *Bioorg. Med. Chem. Lett.* **17**:2310–2311. <http://dx.doi.org/10.1016/j.bmcl.2007.01.059>.
42. Scott SA, Selvy PE, Buck JR, Cho HP, Criswell TL, Thomas AL, Armstrong MD, Arteaga CL, Lindsley CW, Brown HA. 2009. Design of isoform-selective phospholipase D inhibitors that modulate cancer cell invasiveness. *Nat. Chem. Biol.* **5**:108–117. <http://dx.doi.org/10.1038/nchembio.140>.
43. Selvy PE, Lavieri RR, Lindsley CW, Brown HA. 2011. Phospholipase D: enzymology, functionality, and chemical modulation. *Chem. Rev.* **111**: 6064–6119. <http://dx.doi.org/10.1021/cr200296t>.
44. He CY, Shaw MK, Pletcher CH, Striepen B, Tilney LG, Roos DS. 2001. A plastid segregation defect in the protozoan parasite *Toxoplasma gondii*. *EMBO J.* **20**:330–339. <http://dx.doi.org/10.1093/emboj/20.3.330>.
45. Goodman CD, Su V, McFadden GI. 2007. The effects of anti-bacterials on the malaria parasite *Plasmodium falciparum*. *Mol. Biochem. Parasitol.* **152**:181–191. <http://dx.doi.org/10.1016/j.molbiopara.2007.01.005>.
46. Dahl EL, Rosenthal PJ. 2008. Apicoplast translation, transcription and genome replication: targets for antimalarial antibiotics. *Trends Parasitol.* **24**:279–284. <http://dx.doi.org/10.1016/j.pt.2008.03.007>.
47. Dahl EL, Rosenthal PJ. 2007. Multiple antibiotics exert delayed effects against the *Plasmodium falciparum* apicoplast. *Antimicrob. Agents Chemother.* **51**:3485–3490. <http://dx.doi.org/10.1128/AAC.00527-07>.
48. Vial HJ, Thuét MJ, Philippot JR. 1982. Phospholipid biosynthesis in synchronous *Plasmodium falciparum* cultures. *J. Protozool.* **29**:258–263. <http://dx.doi.org/10.1111/j.1550-7408.1982.tb04023.x>.
49. Maréchal E, Azzouz N, de Macedo CS, Block MA, Feagin JE, Schwarz RT, Joyard J. 2002. Synthesis of chloroplast galactolipids in apicomplexan parasites. *Eukaryot. Cell* **1**:653–656. <http://dx.doi.org/10.1128/EC.1.4.653-656.2002>.
50. Ramasamy R, Field MC. 2012. Terminal galactosylation of glycoconjugates in *Plasmodium falciparum* asexual blood stages and *Trypanosoma brucei* bloodstream trypomastigotes. *Exp. Parasitol.* **130**:314–320. <http://dx.doi.org/10.1016/j.exppara.2012.02.017>.
51. Welti R, Mui E, Sparks A, Wernimont S, Isaac G, Kirisits M, Roth M, Roberts CW, Botté C, Maréchal E, McLeod R. 2007. Lipidomic analysis of *Toxoplasma gondii* reveals unusual polar lipids. *Biochemistry* **46**: 13882–13890. <http://dx.doi.org/10.1021/bi7011993>.
52. Peters W. 1975. The chemotherapy of rodent malaria, XXII. The value of drug-resistant strains of *P. berghei* in screening for blood schizontocidal activity. *Ann. Trop. Med. Parasitol.* **69**:155–171.
53. Peters W, Robinson BL. 1992. The chemotherapy of rodent malaria. XLVII. Studies on pyronaridine and other Mannich base antimalarials. *Ann. Trop. Med. Parasitol.* **86**:455–465.

Supplementary information 1

Analyzes of compounds subjected in the present work to an in depth analysis for their potential antiparasitic properties.

Compound (1): (S)-2-(dibenzylamino)-3-phenylpropyl 4-(1,2-dihydro-2-oxobenzo[d]imidazol-3-yl)piperidine-1-carboxylate

White solid (95%)

Flash chromatography on silica gel (cyclohexane/ ethyl acetate 7/3).

¹H NMR (400 MHz, CDCl₃, ppm) 10.49 (s, 1H, NH), 7.30 (m, 12H, Ph), 7.10 (m, 7H, Ph), 4.46 (m, 1H, CHCH₂CH₂N), 4.45 (m, 2H, CHCH₂CH₂N), 4.38 (m, 1H, CH₂O), 4.22 (m, 1H, CH₂O), 3.83 (d, J = 13.8 Hz, 2H, NCH₂Ph), 3.75 (d, J = 13.8 Hz, 2H, NCH₂Ph), 3.30 (m, 1H, CHCH₂Ph), 3.10 (dd, J = 13.6, 5.8 Hz, 1H, CHCH₂Ph), 2.94 (m, 2H, CHCH₂CH₂N), 2.71 (dd, J = 13.6, 8.5 Hz, 1H, CHCH₂Ph), 2.38 (m, 2H, CHCH₂CH₂N), 1.88 (m, 2H, CHCH₂CH₂N).

¹³C NMR (100 MHz, CDCl₃, ppm) δ 155.1, 155.1 (C=O), 139.8, 139.5, 135.0, 129.2, 128.9, 128.8, 128.6, 128.3, 128.3, 128.1, 126.9, 126.8, 126.0, 121.4, 121.1, 121.0, 109.9, 109.3 (CPh), 64.7 (CH₂O), 58.5 (CHCH₂Ph), 54.0 (NCH₂Ph), 50.6 (CHCH₂CH₂N), 43.6 (CHCH₂CH₂N), 34.1 (CHCH₂Ph), 29.2 (CHCH₂CH₂N).

LC/MS (ES⁺) m/z 575.1 (M+H)⁺.

HRMS (ESI+) m/z calcd for C₃₆H₃₉N₄O₃ (M + H)⁺ 575.3022, found 575.3017

Compound (4): O-2-(dibenzylamino)ethyl 4-(1,2-dihydro-2-oxobenzo[d]imidazol-3-yl)piperidine-1-carbothioate

White solid (87%).

Flash chromatography on silica gel (cyclohexane/ethyl acetate 7/3).

¹H NMR (400 MHz, CDCl₃) δ 10.44 (s, 1H, NH), 7.39 (d, J=7.4 Hz, 4H, Ph), 7.31 (t, J=7.4, 4H, Ph), 7.24 (m, 2H, Ph), 7.17 (d, J=6.8 Hz, 1H, Ph), 7.08 (m, 3H, Ph), 5.40 (d, J=13.5 Hz, 1H, CHCH₂CH₂N), 4.71 (d, J=13.5 Hz, 1H, CHCH₂CH₂N), 4.68-4.57 (m, 3H, CHCH₂CH₂N, OCH₂CH₂N), 3.68 (s, 4H, NCH₂Ph), 3.18 (t, J=12.5 Hz, 1H, CHCH₂CH₂N), 2.96 (t, J=12.5 Hz, 1H, CHCH₂CH₂N), 2.88 (t, J=5.6 Hz, 2H, OCH₂CH₂N), 2.49 (dq, J=12.6, 3.9 Hz, 1H, CHCH₂CH₂N), 2.31 (dq, J=12.6, 3.9 Hz, 1H, CHCH₂CH₂N), 1.96 (d, J=12.6 Hz, 1H, CHCH₂CH₂N), 1.89 (d, J=12.6 Hz, 1H, CHCH₂CH₂N).
¹³C NMR (100 MHz, CDCl₃) δ 187.4 (C=S), 155.2 (C=O), 139.3, 128.7, 128.6, 128.2, 128.0, 127.0, 121.5, 121.2, 110.0, 109.3 (C_{Ph}), 69.6 (OCH₂ CH₂N), 58.7 (NCH₂Ph), 51.7 (OCH₂ CH₂N), 50.4 (CHCH₂ CH₂N), 49.5, 44.5 (CHCH₂CH₂N), 29.1, 28.7 (CHCH₂CH₂N).

LC/MS (ES⁺) m/z 500.8 (M+H)⁺.

HRMS (ESI+) m/z calcd for C₂₉H₃₃N₄O₂S (M + H)⁺ 501.2324, found 501.2310

Compound (7): (S)-2-(dibenzylamino)propyl 4-(1,2-dihydro-1-methyl-2-oxobenzo[d]imidazol-3-yl)piperidine-1-carboxylate

White solid (95%).

Flash chromatography on silica gel (cyclohexane/ethyl acetate 1/1).

¹H NMR (400 MHz, CDCl₃) δ 7.38 (d, J=7.3 Hz, 4H, Ph), 7.28 (m, 4H, Ph), 7.21 (m, 2H, Ph), 7.06 (m, 4H, Ph), 4.53 (tt, J=12.4, 3.7 Hz, 1H, CHCH₂CH₂N), 4.49-4.30 (m, 2H, CHCH₂CH₂N), 4.27 (dd, J=11.0, 7.5 Hz, 1H, CH₂O), 4.07 (dd, J=11.0, 5.7 Hz, 1H, CH₂O), 3.76 (d, J=13.9 Hz, 2H, NCH₂Ph), 3.57 (d, J=13.9 Hz, 2H, NCH₂Ph), 3.43 (s, 3H, NCH₃), 3.14 (sext., J=6.7 Hz, 1H, CHCH₃), 2.94 (m, 2H, CHCH₂ CH₂N), 2.31 (m, 2H, CHCH₂CH₂N), 1.86 (d, J=6.8 Hz, 2H, CHCH₂CH₂N), 1.12 (d, J=6.8 Hz, 3H, CHCH₃).

LC/MS (ES⁺) m/z 512.9 (M+H)⁺.

HRMS (ESI+) m/z calcd for C₃₁H₃₇N₄O₃ (M + H)⁺ 513.2866, found 513.2862

Compound (8): (S)-2-(dibenzylamino)propyl 4-(2-oxo-3-phenylsulfonyl-2,3-dihydro-1H-benzo[d]imidazol-1-yl)piperidine-1-carboxylate

White solid (85%).

Flash chromatography on preparative TLC (silica gel, cyclohexane/ethyl acetate 7/3).

^1H NMR (400 MHz, CDCl_3) δ 8.16 (d, $J=7.6$ Hz, 2H, Ph), 8.00 (m, 1H, Ph), 7.67 (t, $J=7.5$ Hz, 1H, Ph), 7.55 (t, $J=7.8$ Hz, 2H, Ph), 7.37 (d, $J=7.3$ Hz, 4H), 7.27 (m, 4H, Ph), 7.18 (m, 4H, Ph), 7.08 (m, 1H, Ph), 4.45-4.19 (m, 4H, $\text{CHCH}_2\text{CH}_2\text{N}$, OCH_2), 4.04 (dd, $J=11.1$, 5.7 Hz, 1H, OCH_2), 3.75 (d, $J=13.9$ Hz, 2H, NCH_2Ph), 3.56 (d, $J=13.9$ Hz, 2H, NCH_2Ph), 3.12 (sext., $J=6.7$ Hz, 1H, CHCH_3), 2.84 (m, 2H, $\text{CHCH}_2\text{CH}_2\text{N}$), 2.27 (m, 2H, $\text{CHCH}_2\text{CH}_2\text{N}$), 1.71 (m, 2H, $\text{CHCH}_2\text{CH}_2\text{N}$), 1.11 (d, $J=6.8$ Hz, 3H, CHCH_3).

^{13}C NMR (100 MHz, CDCl_3) δ 155.1, 150.0 (C=O), 140.2, 137.9, 134.5, 129.1, 128.5, 128.3, 128.1, 128.1, 126.8, 126.1, 124.1, 122.4, 113.2, 109.4 (C_{Ph}), 66.9 (CH_2O), 53.7 (NCH_2Ph), 51.9 (CHCH_3), 51.5 ($\text{CHCH}_2\text{CH}_2\text{N}$), 43.4 ($\text{CHCH}_2\text{CH}_2\text{N}$), 28.6 ($\text{CHCH}_2\text{CH}_2\text{N}$), 11.2 (CHCH_3).

LC/MS (ES^+) m/z 638.9 ($\text{M}+\text{H}$) $^+$.

HRMS (ESI^+) m/z calcd for $\text{C}_{36}\text{H}_{39}\text{N}_4\text{O}_5\text{S}$ ($\text{M} + \text{H}$) $^+$ 639.2641, found 639.2620

Compound (12): (S)-2-(dibenzylamino)propyl 4-(1H-benzo[d]imidazol-2-ylamino)piperidine-1-carboxylate

Colorless oil (82%).

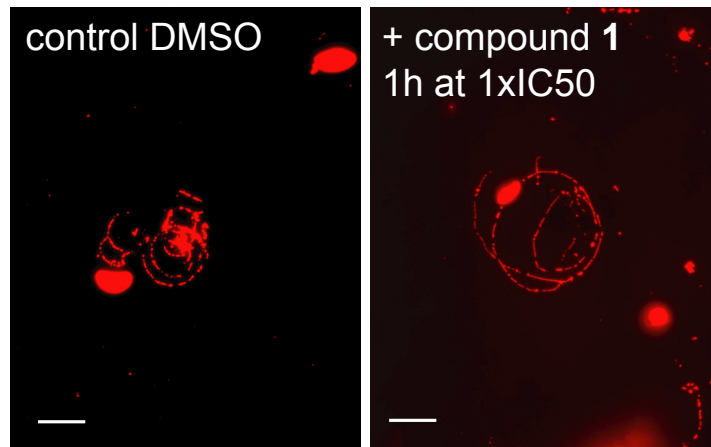
Flash chromatography (silica gel, cyclohexane/ethyl acetate 7/3).

^1H NMR (400 MHz, CDCl_3) δ 7.33 (d, $J=7.6$ Hz, 4H, Bn), 7.27 (m, 6H, Ar), 7.19 (m, 2H, Ar), 7.04 (dd, $J=6.0$, 3.2 Hz, 2H, Ar), 5.12 (s, 1H, NH), 4.19 (m, 1H, CH_2O), 4.03-3.93 (m, 4H, $\text{CHCH}_2\text{CH}_2\text{N}_{\text{pip}}$, $\text{CHCH}_2\text{CH}_2\text{N}_{\text{pip}}$, CH_2O), 3.69 (d, $J=14.0$ Hz, 2H, NCH_2Ph), 3.51 (d, $J=14.0$ Hz, 2H, NCH_2Ph), 3.08 (m, 1H, CHMe), 2.86 (m, 2H, $\text{CHCH}_2\text{CH}_2\text{N}_{\text{pip}}$), 2.05 (m, 2H, $\text{CHCH}_2\text{CH}_2\text{N}_{\text{pip}}$), 1.32 (m, 2H, $\text{CHCH}_2\text{CH}_2\text{N}_{\text{pip}}$), 1.03 (d, $J=6.4$ Hz, 3H, Me).

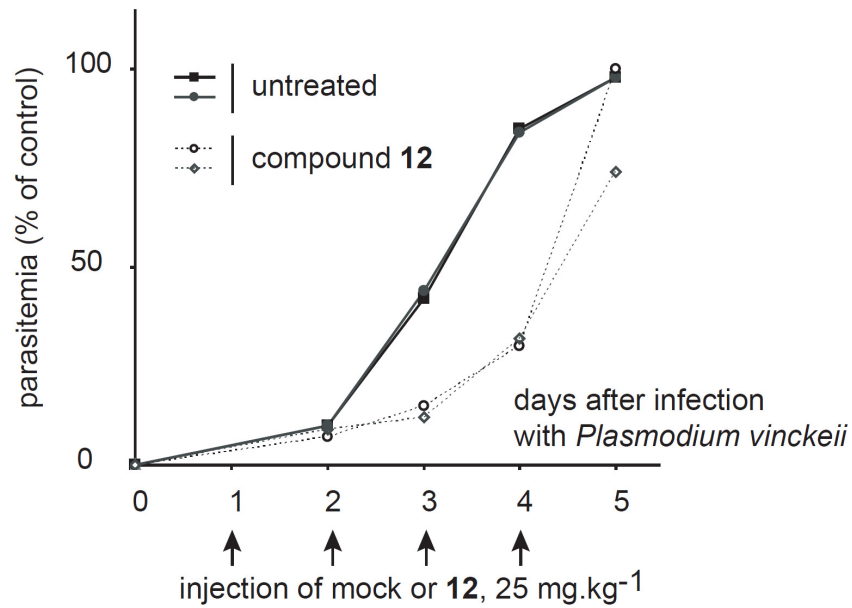
^{13}C NMR (100 MHz, CDCl_3) δ 155.4 (C=O), 153.8 (C=N), 140.1 (C_{Bn}), 137.9 (C_{Ar}), 128.3 (CH_{Bn}), 128.0 (CH_{Bn}), 126.7 (CH_{Bn}), 121.0 (CH_{Ar}), 112.1 (CH_{Ar}), 66.9 (CH_2O), 53.6 (NCH_2Ph), 51.8 (CHMe), 49.8 ($\text{CHCH}_2\text{CH}_2\text{N}_{\text{pip}}$), 42.6 ($\text{CHCH}_2\text{CH}_2\text{N}_{\text{pip}}$), 32.5 ($\text{CHCH}_2\text{CH}_2\text{N}_{\text{pip}}$), 11.0 (Me).

LC/MS (ES^+) m/z 498.3 ($\text{M}+\text{H}$) $^+$.

HRMS (ESI^+) m/z calcd for $\text{C}_{30}\text{H}_{36}\text{N}_5\text{O}_2$ ($\text{M} + \text{H}$) $^+$ 498.2869, found 498.2858



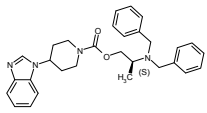
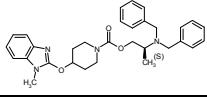
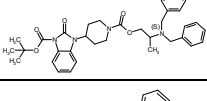
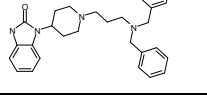
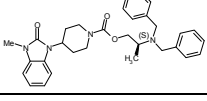
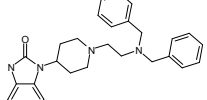
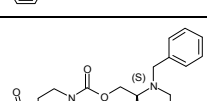
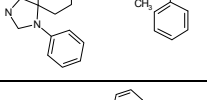
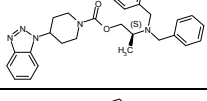
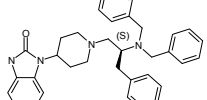
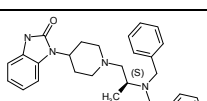
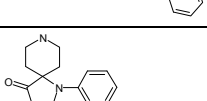
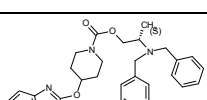
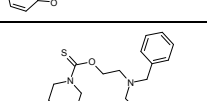
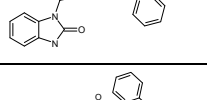
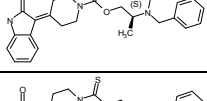
Supplementary Figure 1. Preliminary analysis of the *in vitro* antiparasitic properties of compound 1, harbouring the benzimidazolone-piperidinyl chemotype, on *Toxoplasma gondii*: effect on the motility of free tachyzoites. Motility was tested based on the deposition of SAG1 protein at the surface of glass slides. In both treated and untreated conditions, gliding could be detected for 60% of parasites, with no apparent difference in direction and length.

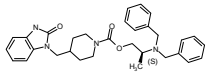
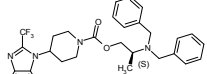
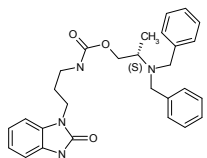
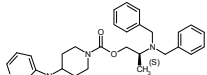
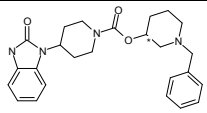
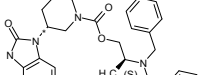
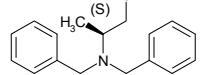
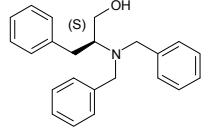
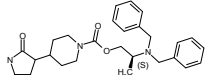
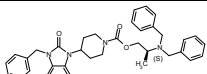
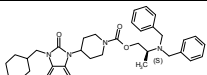
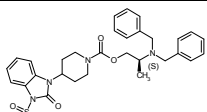
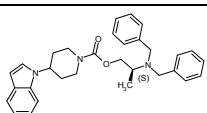
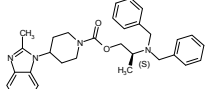
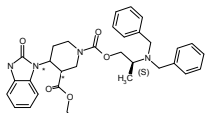
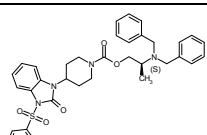


Supplementary Figure 2. Evaluation of the *in vivo* activity of compound 12. Trials were performed after infection of BALB/c mice by *Plasmodium vinckei* (day 0). Compound 12 was supplied by intravenous injection at a concentration of 25 mg.kg⁻¹. Parasitemia was estimated in blood samples at day 0 to 5, in untreated (injection of drug vehicle only) and treated mice. In mice treated with compound 12, development of parasitemia was significantly reduced, but complete cure was not observed

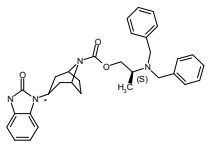
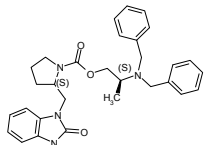
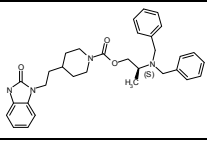
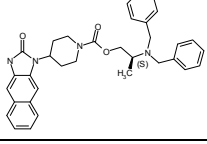
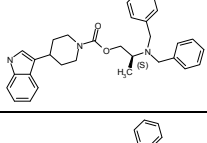
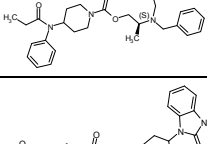
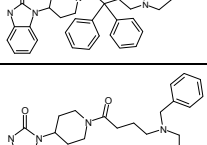
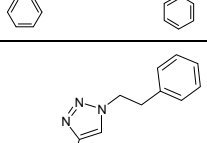
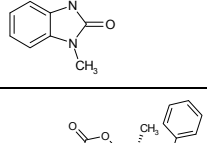
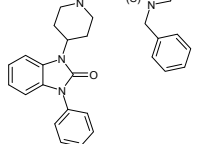
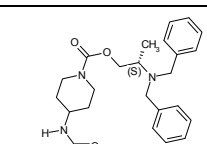
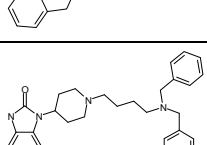
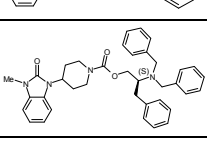
Supplementary Table 1. Evaluation of the *in vitro* antiparasitic properties of 250 compounds designed based on a piperidiny-chemotype interfering with glycerolipid-manipulating enzymes. Compounds have been synthesized and analyzed by liquid chromatography and NMR. Average purity is 93.34% [min 90 - max 99]. Lipinski rules: in average 0.86 H-bond donors [min 0 - max 4]; in average 4.47 H bond acceptors [min 2 - max 9], an average molecular weight of 537 [min 217 - max 844] and an average LogP of 5.18 [min 0.47 - max 9.71]. IC50s have been evaluated as described in Methods and are given in μM . IC50 values are based on three independent experiments for *T. gondii* and two independent experiments for *P. falciparum*, determined graphically from dose-effect curves, with indicated errors, using the Graphpad Prism analytical software. (*), no error estimate for IC50s > 99 μM ; (nt) not tested.

compound identifier	IC50 Toxoplasma (μM)	IC50 Plasmodium (μM)	structure	structure composition	chemical formula	molecular weight
A1B1C1_1	14.0 \pm 0.4	4.9 \pm 0.2		C 72.26% H 6.87% N 11.24% O 9.63%	C30H34N4O3	498.63048
A1B1C2_1	4.8 \pm 0.1	1.4 \pm 0.1		C 75.24% H 6.66% N 9.75% O 8.35%	C36H38N4O3	574.72926
A1B1C3_1	7.5 \pm 0.2	6.9 \pm 0.3		C 71.88% H 6.66% N 11.56% O 9.90%	C29H32N4O3	484.60339
A1B1C4_1	2.5 \pm 0.1	3.6 \pm 0.2		C 72.26% H 6.87% N 11.24% O 9.63%	C30H34N4O3	498.63048
A1B1C5_1	2.0 \pm 0.1	99.0 \pm *		C 64.69% H 6.17% N 13.72% O 11.75%	C23H28N4O3	408.50461
A1B2C1_1	3.5 \pm 0.1	4.1 \pm 0.2		C 72.56% H 6.50% N 11.28% O 9.67%	C30H32N4O3	496.61454
A0B1C1_1	15.0 \pm 0.4	8.0 \pm 0.4		C 75.38% H 8.25% N 7.64% O 8.73%	C23H30N2O2	366.50775
A2B1C1_1	99.0 \pm *	4.3 \pm 0.2		C 78.91% H 7.95% N 6.13% O 7.01%	C30H36N2O2	456.63362
A1B1C8_0	3.0 \pm 0.1	99.0 \pm *		C 71.05% H 8.77% N 14.62% O 5.57%	C17H25N3O	287.4083
A1B1C7_0	99.0 \pm *	99.0 \pm *		C 69.47% H 8.16% N 16.20% O 6.17%	C15H21N3O	259.35412
A1B1C9_0	1.5 \pm 0.0	11.0 \pm 0.6		C 75.83% H 10.61% N 9.83% O 3.74%	C27H45N3O	427.6792
A1B1C0_0	99.0 \pm *	99.0 \pm *		C 66.34% H 6.96% N 19.34% O 7.36%	C12H15N3O	217.27285
A1B1C6_1	0.5 \pm 0.0	99.0 \pm *		C 66.82% H 6.37% N 10.63% O 16.18%	C22H25N3O4	395.46225
A6B1C1_1	3.5 \pm 0.1	1.1 \pm 0.1		C 70.01% H 6.66% N 10.89% O 6.22% S 6.23%	C30H34N4O2S	514.69508
A13B1C1_1	5.2 \pm 0.1	2.1 \pm 0.1		C 71.68% H 6.90% N 7.38% O 14.04%	C34H39N3O5	569.70703

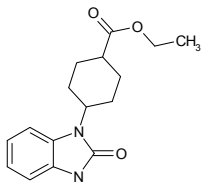
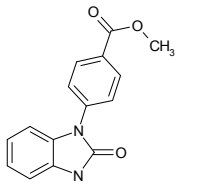
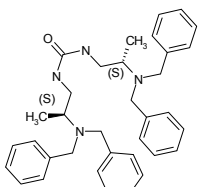
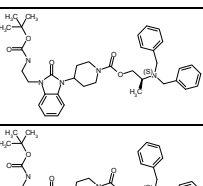
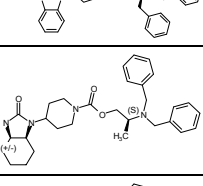
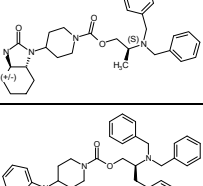
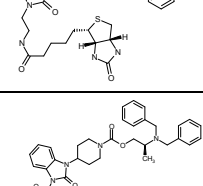
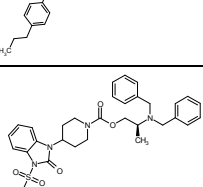
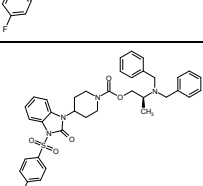
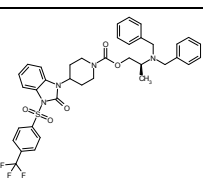

A9B1C1_1	8.0 ± 0.2	1.8 ± 0.1		C 74.66% H 7.10% N 11.61% O 6.63%	C30H34N4O2	482.63108
A4B1C1_1	2.5 ± 0.1	6.2 ± 0.3		C 72.63% H 7.08% N 10.93% O 9.36%	C31H36N4O3	512.65757
A3B1C1_1	2.0 ± 0.1	0.8 ± 0.0		C 70.21% H 7.07% N 9.36% O 13.36%	C35H42N4O5	598.74879
A1B1C4_0	0.8 ± 0.0	1.3 ± 0.1		C 76.62% H 7.54% N 12.32% O 3.52%	C29H34N4O	454.62053
A7B1C1_1	0.2 ± 0.0	1.5 ± 0.1		C 70.29% H 6.49% N 10.93% O 9.36%	C31H36N4O3	512.65757
A1B1C3_0	2.0 ± 0.1	1.6 ± 0.1		C 76.33% H 7.32% N 12.72% O 3.63%	C28H32N4O	440.59344
A5B3C1_1	1.0 ± 0.0	3.8 ± 0.2		C 72.63% H 7.08% N 10.93% O 9.36%	C31H36N4O3	512.65757
A10B1C1_1	4.0 ± 0.1	6.0 ± 0.3		C 72.02% H 6.88% N 14.48% O 6.62%	C29H33N5O2	483.61866
A1B1C2_0	4.0 ± 0.1	2.1 ± 0.1		C 79.21% H 7.22% N 10.56% O 3.01%	C35H38N4O	530.71931
A1B1C1_0	7.0 ± 0.2	3.3 ± 0.2		C 76.62% H 7.54% N 12.32% O 3.52%	C29H34N4O	454.62053
A5B3C0_0	0.5 ± 0.0	15.9 ± 0.8		C 67.51% H 7.41% N 18.17% O 6.92%	C13H17N3O	231.29994
A8B1C1_1	0.8 ± 0.0	14.8 ± 0.7		C 72.12% H 6.66% N 8.41% O 12.81%	C30H33N3O4	499.61521
A1B1C3_2	0.2 ± 0.0	2.8 ± 0.1		C 69.57% H 6.44% N 11.19% O 6.39% S 6.40%	C29H32N4O2S	500.66799
A16B7C1_1	1.4 ± 0.0	3.1 ± 0.2		C 75.13% H 6.71% N 8.48% O 9.68%	C31H33N3O3	495.62696
A1B1C6_2	1.1 ± 0.0	23.2 ± 1.2		C 64.21% H 6.12% N 10.21% O 11.66% S 7.79%	C22H25N3O3S	411.52685
A1B1C1_2	1.2 ± 0.0	3.0 ± 0.1		C 70.01% H 6.66% N 10.89% O 6.22% S 6.23%	C30H34N4O2S	514.69508

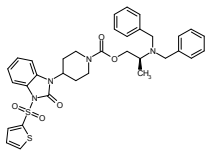
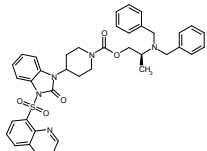
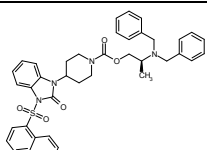
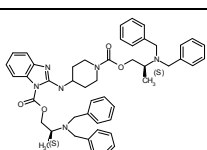
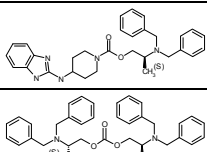
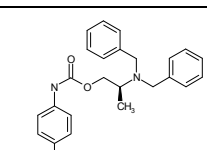
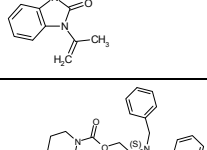
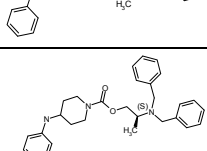
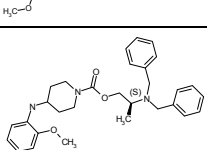
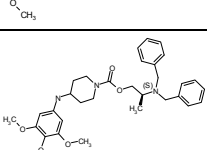
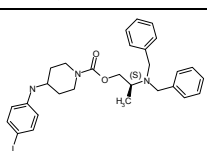
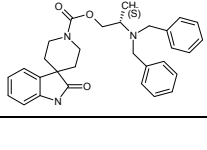

A1B5C1_1	3.4 ± 0.1	5.8 ± 0.3		C 72.63% H 7.08% N 10.93% O 9.36%	C31H36N4O3	512.65757
A15B1C1_1	2.0 ± 0.1	0.8 ± 0.0		C 65.44% H 6.04% N 10.18% O 5.81%	C31H33F3N4O2	550.62946
A1B6C1_1	0.4 ± 0.0	16.6 ± 0.8		C 71.16% H 6.83% N 11.86% O 10.16%	C28H32N4O3	472.59224
A14B1C1_1	2.5 ± 0.1	3.8 ± 0.2		C 69.72% H 6.66% N 14.02% O 9.61%	C29H33N5O3	499.61806
A1B1C10_1	0.5 ± 0.0	25.9 ± 1.3		C 69.10% H 6.96% N 12.89% O 11.05%	C25H30N4O3	434.54285
A1B4C1_1	2.4 ± 0.1	2.8 ± 0.1		C 72.26% H 6.87% N 11.24% O 9.63%	C30H34N4O3	498.63048
A0B0C1_0	1.1 ± 0.0	99.0 ± *		C 79.96% H 8.29% N 5.49% O 6.27%	C17H21NO	255.36302
A0B0C2_0	1.8 ± 0.0	35.1 ± 1.8		C 83.34% H 7.60% N 4.23% O 4.83%	C23H25NO	331.4618
A17B1C1_1	5.6 ± 0.1	3.9 ± 0.2		C 74.82% H 7.09% N 8.44% O 9.65%	C31H35N3O3	497.6429
A18B1C1_1	1.8 ± 0.0	0.8 ± 0.0		C 75.48% H 6.85% N 9.52% O 8.15%	C37H40N4O3	588.75635
A19B1C1_1	1.6 ± 0.0	1.0 ± 0.1		C 74.72% H 7.80% N 9.42% O 8.07%	C37H46N4O3	594.80417
A20B1C1_1	2.0 ± 0.0	1.6 ± 0.1		C 64.56% H 6.29% N 9.71% O 13.87% S 5.56%	C31H36N4O5S	576.72037
A25B1C1_1	0.2 ± 0.0	3.1 ± 0.2		C 77.31% H 7.32% N 8.72% O 6.64%	C31H35N3O2	481.6435
A26B1C1_1	3.4 ± 0.1	2.4 ± 0.1		C 74.97% H 7.31% N 11.28% O 6.44%	C31H36N4O2	496.65817
A1B8C1_1	2.8 ± 0.1	1.5 ± 0.1		C 69.45% H 6.71% N 9.82% O 14.02%	C33H38N4O5	570.69461
A21B1C1_1	1.7 ± 0.0	0.2 ± 0.0		C 67.69% H 6.00% N 8.77% O 12.52% S 5.02%	C36H38N4O5S	638.79206

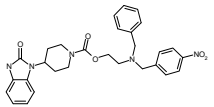
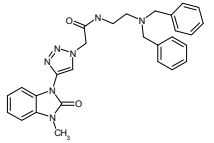
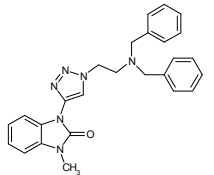
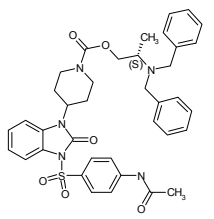
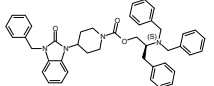
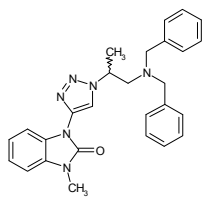
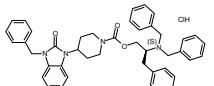
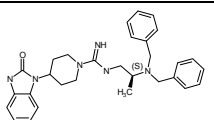
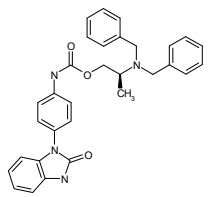
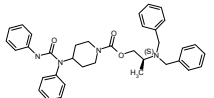
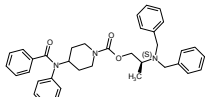
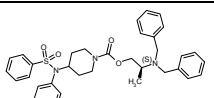
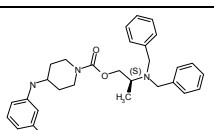
A22B1C1_1	1.0 ± 0.0	2.9 ± 0.1		C 73.73% H 6.35% N 9.30% O 10.62%	C37H38N4O4	602.73981
A23B1C1_1	1.0 ± 0.0	2.9 ± 0.1		C 71.09% H 6.71% N 10.36% O 11.84%	C32H36N4O4	540.66812
A24B1C1_1	2.0 ± 0.0	2.8 ± 0.1		C 76.99% H 7.71% N 8.69% O 6.62%	C31H37N3O2	483.65944
A27B1C1_1	1.0 ± 0.0	4.7 ± 0.2		C 67.60% H 6.24% Cl 6.65% N 10.51% O 9.00%	C30H33ClN4O3	533.07551
A28B1C1_1	25.0 ± 0.6	2.8 ± 0.1		C 77.23% H 7.90% N 8.44% O 6.43%	C32H39N3O2	497.68653
A1B9C1_1	5.0 ± 0.1	10.7 ± 0.5		C 72.63% H 7.08% N 10.93% O 9.36%	C31H36N4O3	512.65757
A1B1C11_1	12.0 ± 0.3	99.0 ± *		C 63.31% H 7.83% N 15.54% O 13.32%	C19H28N4O3	360.46001
A12B1C1_1	2.8 ± 0.1	99.0 ± *		C 72.14% H 7.26% N 9.61% O 10.98%	C35H42N4O4	582.74939
A1B1C17_1	2.0 ± 0.1	2.9 ± 0.1		C 72.18% H 6.27% N 11.61% O 9.95%	C29H30N4O3	482.58745
A1B1C18_1	9.0 ± 0.2	99.0 ± *		C 66.30% H 6.36% N 14.73% O 12.62%	C21H24N4O3	380.45043
A1B1C19_1	27.0 ± 0.7	99.0 ± *		C 64.92% H 8.30% N 14.42% O 12.35%	C21H32N4O3	388.51419
A1B1C12_1	26.0 ± 0.7	99.0 ± *		C 63.59% H 5.10% N 12.90% O 18.41%	C23H22N4O5	434.45559
A1B1C13_1	1.0 ± 0.0	8.2 ± 0.4		C 70.10% H 7.41% N 12.11% O 10.38%	C27H34N4O3	462.59703
A1B1C14_1	1.8 ± 0.0	24.4 ± 1.2		C 67.63% H 6.91% N 13.72% O 11.75%	C23H28N4O3	408.50461
A1B1C16_1	5.0 ± 0.1	18.8 ± 0.9		C 69.10% H 6.96% N 12.89% O 11.05%	C25H30N4O3	434.54285
A1B1C20_1	4.0 ± 0.1	99.0 ± *		C 61.43% H 7.28% N 16.85% O 14.44%	C17H24N4O3	332.40583
A1B1C21_1	1.2 ± 0.0	8.5 ± 0.4		C 73.82% H 6.42% N 9.22% O 10.54%	C28H29N3O3	455.56163
A1B1C22_1	1.0 ± 0.0	1.3 ± 0.1		C 65.18% H 6.36% N 14.38% O 14.08%	C37H43N7O6	681.79856
A1B10C1_1	3.3 ± 0.1	7.2 ± 0.4		C 71.88% H 6.66% N 11.56% O 9.90%	C29H32N4O3	484.60339

A1B11C1_1	7.0 ± 0.2	2.6 ± 0.1		C 73.26% H 6.92% N 10.68% O 9.15%	C32H36N4O3	524.66872
A1B13C1_1	3.1 ± 0.1	7.3 ± 0.4		C 72.26% H 6.87% N 11.24% O 9.63%	C30H34N4O3	498.63048
A1B12C1_1	4.2 ± 0.1	6.8 ± 0.3		C 72.98% H 7.27% N 10.64% O 9.11%	C32H38N4O3	526.68466
A29B1C1_1	0.8 ± 0.0	7.2 ± 0.4		C 74.43% H 6.61% N 10.21% O 8.75%	C34H36N4O3	548.69102
A30B1C1_1	1.9 ± 0.0	5.2 ± 0.3		C 77.31% H 7.32% N 8.72% O 6.64%	C31H35N3O2	481.6435
A31B1C1_1	1.3 ± 0.0	7.2 ± 0.4		C 74.82% H 7.65% N 8.18% O 9.34%	C32H39N3O3	513.68593
A1B1C23_3	1.2 ± 0.0	7.0 ± 0.4		C 73.37% H 6.47% N 12.83% O 7.33%	C40H42N6O3	654.81914
A1B1C24_3	6.3 ± 0.2	11.3 ± 0.6		C 74.66% H 7.10% N 11.61% O 6.63%	C30H34N4O2	482.63108
A7B14C25_0	99.0 ± *	99.0 ± *		C 67.70% H 5.37% N 21.93% O 5.01%	C18H17N5O	319.36909
A32B1C1_1	3.5 ± 0.1	2.3 ± 0.1		C 75.24% H 6.66% N 9.75% O 8.35%	C36H38N4O3	574.72926
A33B1C1_1	4.9 ± 0.1	25.4 ± 1.3		C 74.52% H 7.46% N 8.41% O 9.61%	C31H37N3O3	499.65884
A1B1C26_0	1.5 ± 0.0	3.0 ± 0.1		C 76.89% H 7.74% N 11.95% O 3.41%	C30H36N4O	468.64762
A7B1C2_1	0.8 ± 0.0	0.5 ± 0.0		C 73.44% H 6.33% N 9.52% O 8.15%	C37H40N4O3	588.75635

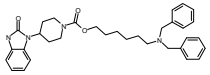
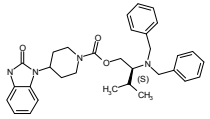
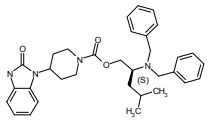
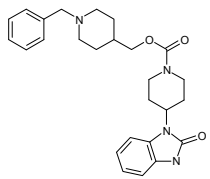
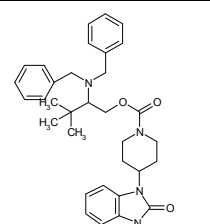
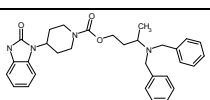
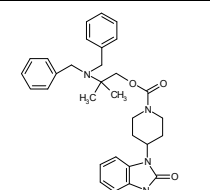
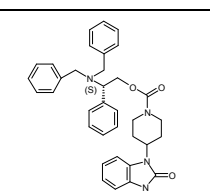
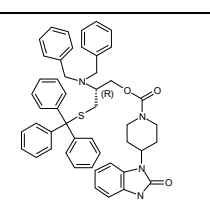
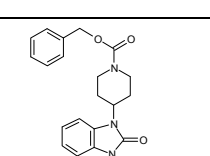
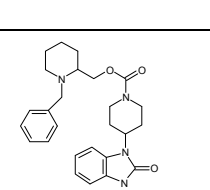
A21B1C2_1	22.0 ± 0.6	1.9 ± 0.1		C 70.57% H 5.92% N 7.84% O 11.19% S 4.49%	C42H42N4O5S	714.89084
A37B3C29_0	99.0 ± *	99.0 ± *		C 78.05% H 6.90% N 9.58% O 5.47%	C19H20N2O	292.38405
A1B1C1_4	15.0 ± 0.4	3.5 ± 0.2		C 72.41% H 7.09% N 14.07% O 6.43%	C30H35N5O2	497.64575
A1B1C1_5	7.5 ± 0.2	2.7 ± 0.1		C 70.14% H 6.87% N 13.63% O 3.11% S 6.24%	C30H35N5OS	513.71035
A1B1C1_3	10.5 ± 0.3	4.0 ± 0.2		C 74.97% H 7.31% N 11.28% O 6.44%	C31H36N4O2	496.65817
A11B1C1_1	11.0 ± 0.3	3.6 ± 0.2		C 74.82% H 7.09% N 8.44% O 9.65%	C31H35N3O3	497.6429
A34B1C1_1	5.7 ± 0.1	0.6 ± 0.0		C 70.56% H 7.24% N 9.14% O 13.05%	C36H44N4O5	612.77588
A35B1C1_1	1.7 ± 0.0	6.3 ± 0.3		C 69.84% H 6.90% N 9.58% O 13.68%	C34H40N4O5	584.7217
A36B1C1_1	11.5 ± 0.3	3.1 ± 0.2		C 72.06% H 6.76% N 9.89% O 11.29%	C34H38N4O4	566.70636
A1B1C15_1	12.0 ± 0.3	8.3 ± 0.4		C 73.45% H 6.16% N 9.52% O 10.87%	C27H27N3O3	441.53454

A1B15C27_1	99.0 ± *	99.0 ± *		C 66.65% H 6.99% N 9.72% O 16.65%	C16H20N2O3	288.3494
A1B16C28_1	99.0 ± *	99.0 ± *		C 67.16% H 4.51% N 10.44% O 17.89%	C15H12N2O3	268.27449
A0B17C1_4	9.2 ± 0.2	1.3 ± 0.1		C 78.61% H 7.92% N 10.48% O 2.99%	C35H42N4O	534.75119
A38B1C1_1	3.0 ± 0.1	1.4 ± 0.1		C 69.24% H 7.38% N 10.91% O 12.46%	C37H47N5O5	641.81764
A38B1C2_1	3.2 ± 0.1	0.4 ± 0.0		C 71.94% H 7.16% N 9.76% O 11.14%	C43H51N5O5	717.91642
A40B1C1_1	2.6 ± 0.1	2.9 ± 0.1		C 71.40% H 7.99% N 11.10% O 9.51%	C30H40N4O3	504.6783
A39B1C1_1	17.0 ± 0.4	3.3 ± 0.2		C 71.40% H 7.99% N 11.10% O 9.51%	C30H40N4O3	504.6783
A41B1C2_1	2.6 ± 0.1	0.5 ± 0.0		C 68.30% H 6.81% N 11.62% O 9.48% S 3.80%	C48H57N7O5S	844.09739
A42B1C1_1	5.5 ± 0.1	9.1 ± 0.5		C 68.80% H 6.51% N 8.23% O 11.75% S 4.71%	C39H44N4O5S	680.87333
A43B1C1_1	1.5 ± 0.0	0.3 ± 0.0		C 65.84% H 5.68% F 2.89% N 8.53% O 12.18% S 4.88%	C36H37FN4O5S	656.78249
A44B1C1_1	1.8 ± 0.0	0.4 ± 0.0		C 66.45% H 6.03% N 8.38% O 14.35% S 4.79%	C37H40N4O6S	668.81855
A45B1C1_1	8.5 ± 0.2	0.4 ± 0.0		C 62.88% H 5.28% F 8.06% N 7.93% O 11.32% S 4.54%	C37H37F3N4O5S	706.79044

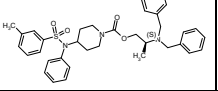
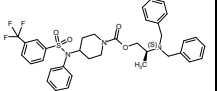
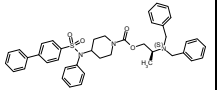
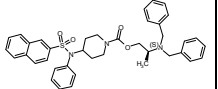
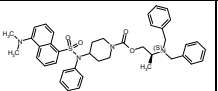
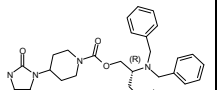
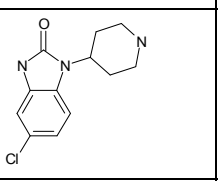
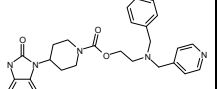
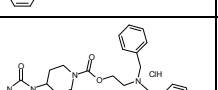
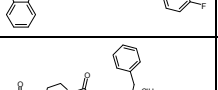
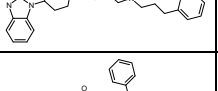
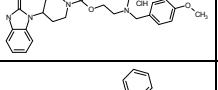
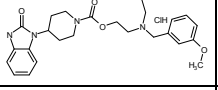
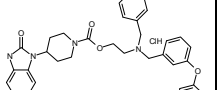
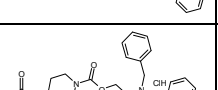
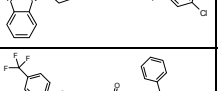
A46B1C1_1	3.8 ± 0.1	0.5 ± 0.0		C 63.33% H 5.63% N 8.69% O 12.41% S 9.95%	C34H36N4O5S2	644.81782
A47B1C1_1	99.0 ± *	0.8 ± 0.0		C 67.90% H 5.70% N 10.15% O 11.60% S 4.65%	C39H39N5O5S	689.84018
A48B1C1_1	2.3 ± 0.1	1.0 ± 0.0		C 69.75% H 5.85% N 8.13% O 11.61% S 4.65%	C40H40N4O5S	688.8526
A50B1C1_1	9.0 ± 0.2	2.6 ± 0.1		C 74.01% H 6.99% N 10.79% O 8.22%	C48H54N6O4	779.00338
A51B1C1_1	1.0 ± 0.0	0.2 ± 0.0		C 72.41% H 7.09% N 14.07% O 6.43%	C30H35N5O2	497.64575
A0B19C1_1	12.0 ± 0.3	1.6 ± 0.1		C 78.33% H 7.51% N 5.22% O 8.94%	C35H40N2O3	536.72065
A52B18C1_1	6.0 ± 0.2	3.3 ± 0.2		C 74.70% H 6.27% N 10.25% O 8.78%	C34H34N4O3	546.67508
A53B1C1_1	9.5 ± 0.2	3.4 ± 0.2		C 76.12% H 7.71% N 9.18% O 6.99%	C29H35N3O2	457.6212
A54B1C1_1	10.0 ± 0.3	8.4 ± 0.4		C 73.89% H 7.65% N 8.62% O 9.84%	C30H37N3O3	487.64769
A55B1C1_1	7.3 ± 0.2	2.4 ± 0.1		C 71.93% H 7.59% N 8.12% O 12.36%	C31H39N3O4	517.67418
A56B1C1_1	16.0 ± 0.4	3.1 ± 0.2		C 70.18% H 7.55% N 7.67% O 14.61%	C32H41N3O5	547.70067
A57B1C1_1	7.7 ± 0.2	8.1 ± 0.4		C 59.69% H 5.87% I 21.75% N 7.20% O 5.48%	C29H34IN3O2	583.51763
A49B3C1_1	7.5 ± 0.2	3.9 ± 0.2		C 74.51% H 6.88% N 8.69% O 9.92%	C30H33N3O3	483.61581

A1B1C30_1	3.3 ± 0.1	3.0 ± 0.2		C 65.77% H 5.90% N 10.58% O 9.06%	C29H31N5O5	529.60092
A7B14C31_0	14.8 ± 0.4	24.5 ± 1.2		C 67.86% H 5.90% N 19.78% O 6.46%	C28H29N7O2	495.58903
A7B14C3_0	50.0 ± 1.3	10.8 ± 0.5		C 71.21% H 5.98% N 19.16% O 3.65%	C26H26N6O	438.53672
A58B1C1_1	3.0 ± 0.1	1.5 ± 0.1		C 65.59% H 5.94% N 10.06% O 13.80% S 4.61%	C38H41N5O6S	695.84437
A18B1C2_1	3.6 ± 0.1	1.0 ± 0.0		C 77.68% H 6.67% N 8.43% O 7.22%	C43H44N4O3	664.85513
A7B14C32_0	7.5 ± 0.2	7.6 ± 0.4		C 71.66% H 6.24% N 18.57% O 3.54%	C27H28N6O	452.56381
A18B1C33_1	1.8 ± 0.0	0.9 ± 0.0		C 73.64% H 6.47% Cl 5.06% N 7.99% O 6.84%	C43H45ClN4O3	701.3161
A1B1C1_6	11.0 ± 0.3	0.5 ± 0.0		C 72.55% H 7.31% N 16.92% O 3.22%	C30H36N6O	496.66102
A1B18C1_1	5.0 ± 0.1	7.9 ± 0.4		C 73.50% H 5.97% N 11.06% O 9.47%	C31H30N4O3	506.60975
A62B1C1_1	2.7 ± 0.1	4.1 ± 0.2		C 74.97% H 6.99% N 9.71% O 8.32%	C36H40N4O3	576.7452
A63B1C1_1	2.7 ± 0.1	1.5 ± 0.1		C 76.98% H 7.00% N 7.48% O 8.54%	C36H39N3O3	561.73053
A64B1C1_1	1.8 ± 0.0	0.5 ± 0.0		C 70.32% H 6.58% N 7.03% O 10.71% S 5.36%	C35H39N3O4S	597.78278
A59B1C1_1	5.5 ± 0.1	6.7 ± 0.3		C 73.24% H 7.21% F 3.99% N 8.83% O 6.73%	C29H34FN3O2	475.61163

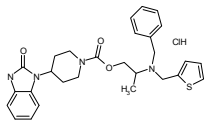
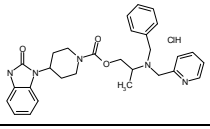
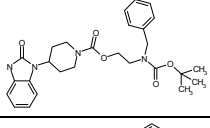
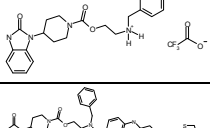
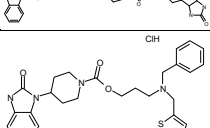
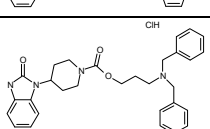
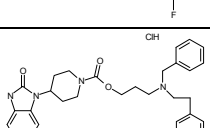
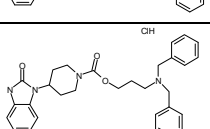
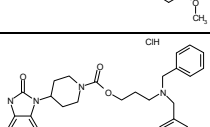
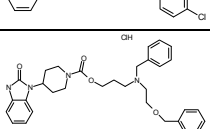
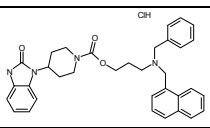
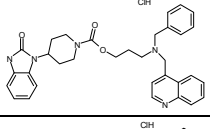
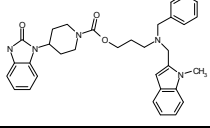
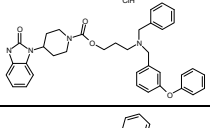
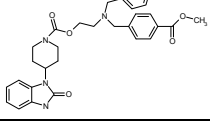

A60B1C1_1	3.8 ± 0.1	7.3 ± 0.4		C 66.16% H 6.32% Cl 13.47% N 7.98% O 6.08%	C29H33Cl2N3O2	526.51126
A61B1C1_1	12.9 ± 0.3	10.3 ± 0.5		C 73.70% H 7.68% N 11.85% O 6.77%	C29H36N4O2	472.63587
A65B1C1_1	1.7 ± 0.0	7.0 ± 0.3		C 70.70% H 6.51% N 10.64% O 12.15%	C31H34N4O4	526.64103
A66B1C1_1	3.8 ± 0.1	2.3 ± 0.1		C 77.39% H 6.86% N 10.03% O 5.73%	C36H38N4O2	558.72986
A67B1C1_1	3.8 ± 0.1	36.5 ± 1.8		C 72.41% H 7.09% N 14.07% O 6.43%	C30H35N5O2	497.64575
A68B1C1_1	6.9 ± 0.2	1.6 ± 0.1		C 71.33% H 7.09% N 6.57% O 10.00% S 5.01%	C38H45N3O4S	639.86405
A69B1C1_1	0.8 ± 0.0	0.6 ± 0.0		C 68.27% H 6.22% F 3.09% N 6.82% O 10.39% S 5.21%	C35H38FN3O4S	615.77321
A70B1C1_1	4.0 ± 0.1	0.8 ± 0.0		C 66.96% H 6.10% N 6.69% O 10.19% S 5.11%	C36H41N3O5S	627.80927
A71B1C1_1	5.5 ± 0.1	0.4 ± 0.0		C 64.95% H 5.75% F 8.56% N 6.31% O 9.61% S 4.82%	C36H38F3N3O4S	665.78116
A72B1C1_1	1.0 ± 0.0	0.9 ± 0.0		C 65.64% H 6.18% N 6.96% O 10.60% S 10.62%	C33H37N3O4S2	603.80854
A73B1C1_1	2.7 ± 0.1	1.1 ± 0.1		C 70.35% H 6.21% N 8.64% O 9.86% S 4.94%	C38H40N4O4S	648.8309
A74B1C1_1	6.0 ± 0.2	0.3 ± 0.0		C 72.31% H 6.38% N 6.49% O 9.88% S 4.95%	C39H41N3O4S	647.84332
A1B1C34_1	2.3 ± 0.1	3.0 ± 0.2		C 74.70% H 6.27% N 10.25% O 8.78%	C34H34N4O3	546.67508
A1B1C35_1	1.3 ± 0.0	8.5 ± 0.4		C 74.41% H 6.06% N 10.52% O 9.01%	C33H32N4O3	532.64799
A75B1C1_1	3.7 ± 0.1	3.0 ± 0.1		C 75.38% H 8.00% N 7.76% O 8.86%	C34H43N3O3	541.74011
A76B1C1_1	3.3 ± 0.1	7.0 ± 0.4		C 72.26% H 6.87% N 11.24% O 9.63%	C30H34N4O3	498.63048

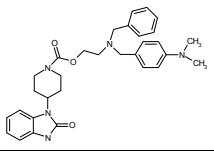
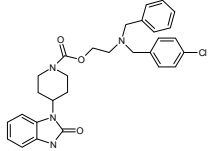
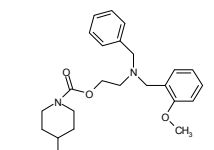
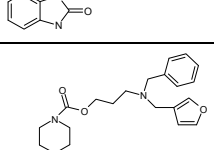
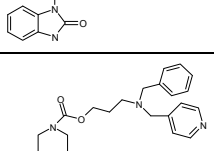
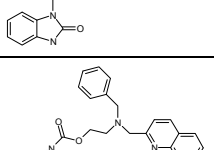
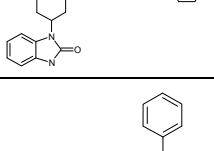
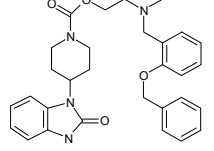
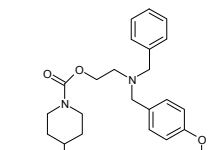
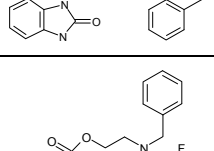
A1B1C36_1	2.0 ± 0.1	2.7 ± 0.1		C 73.30% H 7.46% N 10.36% O 8.88%	C33H40N4O3	540.71175
A1B1C37_1	7.0 ± 0.2	2.8 ± 0.1		C 72.98% H 7.27% N 10.64% O 9.11%	C32H38N4O3	526.68466
A1B1C38_1	3.8 ± 0.1	2.6 ± 0.1		C 73.30% H 7.46% N 10.36% O 8.88%	C33H40N4O3	540.71175
A1B1C39_1	20.0 ± 0.5	25.4 ± 1.3		C 69.62% H 7.19% N 12.49% O 10.70%	C26H32N4O3	448.56994
A1B1C40_1	8.0 ± 0.2	2.4 ± 0.1		C 73.30% H 7.46% N 10.36% O 8.88%	C33H40N4O3	540.71175
A1B1C41_1	3.6 ± 0.1	1.5 ± 0.1		C 72.63% H 7.08% N 10.93% O 9.36%	C31H36N4O3	512.65757
A1B1C42_1	5.1 ± 0.1	2.3 ± 0.1		C 72.63% H 7.08% N 10.93% O 9.36%	C31H36N4O3	512.65757
A1B1C43_1	3.8 ± 0.1	0.5 ± 0.0		C 74.98% H 6.47% N 9.99% O 8.56%	C35H36N4O3	560.70217
A1B1C44_1	17.5 ± 0.4	7.4 ± 0.4		C 76.14% H 6.26% N 7.25% O 6.21% S 4.15%	C49H48N4O3S	773.01791
A1B1C45_1	0.3 ± 0.0	77.2 ± 3.9		C 68.36% H 6.02% N 11.96% O 13.66%	C20H21N3O3	351.40867
A1B1C46_1	5.0 ± 0.1	6.4 ± 0.3		C 69.62% H 7.19% N 12.49% O 10.70%	C26H32N4O3	448.56994

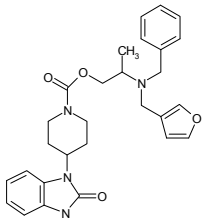
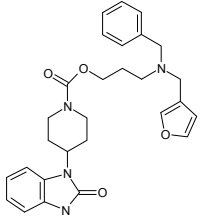
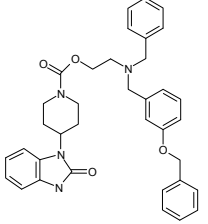
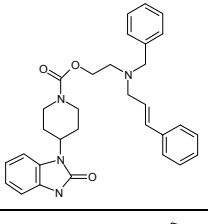
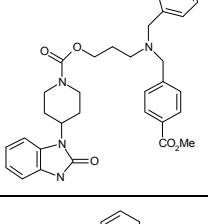
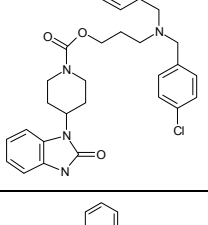
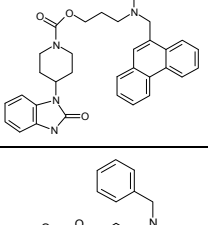
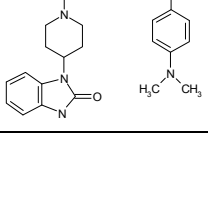
A1B1C47_1	7.5 ± 0.2	6.2 ± 0.3		C 71.47% H 6.43% N 11.91% O 10.20%	C28H30N4O3	470.5763
A1B1C48_1	2.0 ± 0.1	2.2 ± 0.1		C 73.58% H 7.11% N 10.40% O 8.91%	C33H38N4O3	538.69581
A77B1C1_1	39.0 ± 1.0	1.3 ± 0.1		C 70.32% H 6.58% N 7.03% O 10.71% S 5.36%	C35H39N3O4S	597.78278
A78B1C1_1	9.5 ± 0.2	4.5 ± 0.2		C 71.43% H 6.82% N 8.62% O 6.56% S 6.57%	C29H33N3O2S	487.66926
A79B1C1_1	3.0 ± 0.1	1.3 ± 0.1		C 72.94% H 6.80% N 9.45% O 5.40% S 5.41%	C36H40N4O2S	592.8098
A80B1C1_1	6.3 ± 0.2	5.3 ± 0.3		C 72.70% H 7.63% N 10.60% O 9.08%	C32H40N4O3	528.7006
A81B1C1_1	12.0 ± 0.3	3.7 ± 0.2		C 76.40% H 7.91% N 8.91% O 6.78%	C30H37N3O2	471.64829
A1B1C49_1	9.0 ± 0.2	2.5 ± 0.1		C 62.12% H 5.91% Cl 6.11% N 9.66% O 8.27%	C30H34ClN5O5	580.08898
A1B1C50_1	3.3 ± 0.1	3.2 ± 0.2		C 62.12% H 5.91% Cl 6.11% N 9.66% O 8.27%	C30H34ClN5O5	580.08898
A1B1C51_1	6.6 ± 0.2	99.0 ± 5.0		C 65.89% H 6.60% Cl 6.27% N 9.91% O 11.32%	C31H37ClN4O4	565.11794
A1B1C52_1	3.2 ± 0.1	4.4 ± 0.2		C 58.06% H 5.38% Br 13.32% Cl 5.91% N 9.34% O 8.00%	C29H32BrClN4O3	599.96039
A1B1C53_1	11.5 ± 0.3	2.9 ± 0.1		C 58.69% H 5.58% Br 13.01% Cl 5.77% N 9.13% O 7.82%	C30H34BrClN4O3	613.98748
A1B1C54_1	5.5 ± 0.1	1.9 ± 0.1		C 65.89% H 6.60% Cl 6.27% N 9.91% O 11.32%	C31H37ClN4O4	565.11794
A53B1C2_1	3.8 ± 0.1	0.9 ± 0.0		C 78.77% H 7.37% N 7.87% O 6.00%	C35H39N3O2	533.71998
A82B1C1_1	3.9 ± 0.1	0.3 ± 0.0		C 70.68% H 6.76% N 6.87% O 10.46% S 5.24%	C36H41N3O4S	611.80987

A83B1C1_1	2.9 ± 0.1	0.5 ± 0.0		C 70.68% H 6.76% N 6.87% O 10.46% S 5.24%	C36H41N3O4S	611.80987
A84B1C1_1	3.2 ± 0.1	0.6 ± 0.0		C 64.95% H 5.75% F 8.56% N 6.31% O 9.61% S 4.82%	C36H38F3N3O4S	665.78116
A85B1C1_1	6.2 ± 0.2	2.2 ± 0.1		C 73.08% H 6.43% N 6.24% O 9.50% S 4.76%	C41H43N3O4S	673.88156
A86B1C1_1	13.2 ± 0.3	4.4 ± 0.2		C 72.31% H 6.38% N 6.49% O 9.88% S 4.95%	C39H41N3O4S	647.84332
A87B1C1_1	0.2 ± 0.0	0.3 ± 0.0		C 71.28% H 6.71% N 8.11% O 9.26% S 4.64%	C41H46N4O4S	690.91217
A1B1C56_1	2.9 ± 0.1	1.5 ± 0.1		C 75.24% H 6.66% N 9.75% O 8.35%	C36H38N4O3	574.72926
A27B1C0_0	99.0 ± *	99.0 ± *		C 57.26% H 5.61% Cl 14.08% N 16.69% O 6.36%	C12H14ClN3O	251.71788
A1B1C55_1	18.8 ± 0.5	12.5 ± 0.6		C 69.26% H 6.44% N 14.42% O 9.88%	C28H31N5O3	485.59097
A1B1C57_1	1.4 ± 0.0	3.6 ± 0.2		C 64.62% H 5.98% Cl 6.58% F 3.52% N 10.39% O 8.90%	C29H32ClFN4O3	539.05479
A1B1C58_1	1.7 ± 0.0	3.6 ± 0.2		C 67.81% H 6.79% Cl 6.46% N 10.20% O 8.74%	C31H37ClN4O3	549.11854
A1B1C59_1	5.0 ± 0.1	3.5 ± 0.2		C 65.39% H 6.40% Cl 6.43% N 10.17% O 11.61%	C30H35ClN4O4	551.09085
A1B1C60_1	1.8 ± 0.0	3.7 ± 0.2		C 65.39% H 6.40% Cl 6.43% N 10.17% O 11.61%	C30H35ClN4O4	551.09085
A1B1C61_1	3.7 ± 0.1	1.4 ± 0.1		C 68.56% H 6.08% Cl 5.78% N 9.14% O 10.44%	C35H37ClN4O4	613.16254
A1B1C62_1	5.3 ± 0.1	3.3 ± 0.2		C 62.70% H 5.81% Cl 12.76% N 10.09% O 8.64%	C29H32Cl2N4O3	555.50939
A71B1C2_1	3.1 ± 0.1	1.6 ± 0.1		C 68.00% H 5.71% F 7.68% N 5.66% O 8.63% S 4.32%	C42H42F3N3O4S	741.87994
A74B1C2_1	5.5 ± 0.1	1.3 ± 0.1		C 74.66% H 6.27% N 5.80% O 8.84% S 4.43%	C45H45N3O4S	723.9421

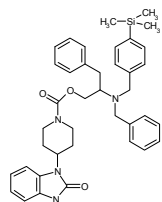
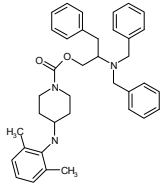
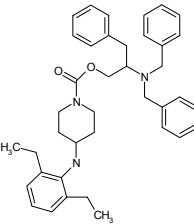
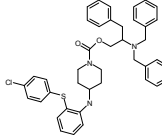
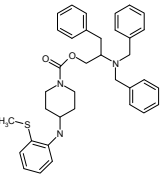
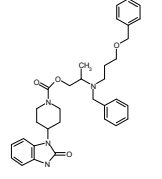
A70B1C2_1	6.3 ± 0.2	0.8 ± 0.0		C 71.67% H 6.44% N 5.97% O 11.36% S 4.56%	C42H45N3O5S	703.90805
A1B1C63_1	3.3 ± 0.1	5.9 ± 0.3		C 65.15% H 6.20% Cl 6.41% F 3.44% N 10.13% O 8.68%	C30H34ClFN4O3	553.08188
A1B1C64_1	4.0 ± 0.1	4.2 ± 0.2		C 68.25% H 6.98% Cl 6.30% N 9.95% O 8.52%	C32H39ClN4O3	563.14563
A1B1C72_1	1.0 ± 0.0	2.6 ± 0.1		C 67.62% H 6.19% Cl 6.05% N 11.95% O 8.19%	C33H36ClN5O3	586.13957
A1B1C65_1	3.8 ± 0.1	4.0 ± 0.2		C 65.89% H 6.60% Cl 6.27% N 9.91% O 11.32%	C31H37ClN4O4	565.11794
A1B1C66_1	5.2 ± 0.1	2.7 ± 0.1		C 68.94% H 6.27% Cl 5.65% N 8.93% O 10.20%	C36H39ClN4O4	627.18963
A1B1C67_1	5.0 ± 0.1	2.1 ± 0.1		C 63.27% H 6.02% Cl 12.45% N 9.84% O 8.43%	C30H34Cl2N4O3	569.53648
A1B1C68_1	7.6 ± 0.2	3.6 ± 0.2		C 63.27% H 6.02% Cl 12.45% N 9.84% O 8.43%	C30H34Cl2N4O3	569.53648
A1B1C69_1	7.2 ± 0.2	3.9 ± 0.2		C 69.40% H 6.18% Cl 6.21% N 9.81% O 8.40%	C33H35ClN4O3	571.1249
A1B1C70_1	1.1 ± 0.0	3.0 ± 0.1		C 67.18% H 5.99% Cl 6.20% N 12.24% O 8.39%	C32H34ClN5O3	572.11248
A1B1C71_1	1.2 ± 0.0	4.2 ± 0.2		C 66.95% H 6.32% Cl 6.18% N 12.20% O 8.36%	C32H36ClN5O3	574.12842
A1B1C73_1	7.0 ± 0.2	1.1 ± 0.1		C 64.98% H 6.39% Cl 6.61% N 13.06% O 8.95%	C29H34ClN5O3	536.07903
A1B1C74_1	2.3 ± 0.1	1.6 ± 0.1		C 64.98% H 6.39% Cl 6.61% N 13.06% O 8.95%	C29H34ClN5O3	536.07903
A1B1C75_1	0.8 ± 0.0	1.2 ± 0.1		C 69.31% H 6.45% Cl 5.53% N 8.74% O 9.98%	C37H41ClN4O4	641.21672
A1B1C76_1	0.7 ± 0.0	1.5 ± 0.1		C 71.85% H 6.19% Cl 5.58% N 8.82% O 7.56%	C38H39ClN4O3	635.21253
A1B1C78_1	3.8 ± 0.1	1.4 ± 0.1		C 69.79% H 6.37% Cl 6.06% N 9.57% O 8.20%	C34H37ClN4O3	585.15199

A1B1C79_1	5.0 ± 0.1	2.7 ± 0.1		C 62.15% H 6.15% Cl 6.55% N 10.35% O 8.87% S 5.93%	C28H33ClN4O3S	541.11721
A1B1C80_1	1.8 ± 0.0	2.5 ± 0.1		C 64.98% H 6.39% Cl 6.61% N 13.06% O 8.95%	C29H34ClN5O3	536.07903
A1B1C82_1	2.0 ± 0.1	4.3 ± 0.2		C 65.57% H 6.93% N 11.33% O 16.17%	C27H34N4O5	494.59583
A1B1C83_1	17.5 ± 0.4	10.0 ± 0.5		C 60.65% H 5.98% N 12.30% O 21.08%	C23H27N4O6	455.49484
A1B1C84_1	11.5 ± 0.3	1.3 ± 0.1		C 64.53% H 6.53% N 13.51% O 11.02% S 4.42%	C39H47N7O5S	725.91734
A1B1C81_1	4.0 ± 0.1	2.1 ± 0.1		C 62.15% H 6.15% Cl 6.55% N 10.35% O 8.87% S 5.93%	C28H33ClN4O3S	541.11721
A1B1C91_1	5.3 ± 0.1	2.2 ± 0.1		C 65.15% H 6.20% Cl 6.41% F 3.44% N 10.13% O 8.68%	C30H34ClFN4O3	553.08188
A1B1C92_1	6.0 ± 0.2	4.6 ± 0.2		C 67.81% H 6.79% Cl 6.46% N 10.20% O 8.74%	C31H37ClN4O3	549.11854
A1B1C93_1	3.5 ± 0.1	0.6 ± 0.0		C 65.89% H 6.60% Cl 6.27% N 9.91% O 11.32%	C31H37ClN4O4	565.11794
A1B1C85_1	1.2 ± 0.0	2.9 ± 0.1		C 63.27% H 6.02% Cl 12.45% N 9.84% O 8.43%	C30H34Cl2N4O3	569.53648
A1B1C86_1	7.0 ± 0.2	4.3 ± 0.2		C 66.37% H 6.79% Cl 6.12% N 9.67% O 11.05%	C32H39ClN4O4	579.14503
A1B1C87_1	2.7 ± 0.1	3.2 ± 0.2		C 69.79% H 6.37% Cl 6.06% N 9.57% O 8.20%	C34H37ClN4O3	585.15199
A1B1C88_1	3.3 ± 0.1	0.7 ± 0.0		C 67.62% H 6.19% Cl 6.05% N 11.95% O 8.19%	C33H36ClN5O3	586.13957
A1B1C89_1	4.8 ± 0.1	9.0 ± 0.5		C 67.39% H 6.51% Cl 6.03% N 11.91% O 8.16%	C33H38ClN5O3	588.15551
A1B1C90_1	1.5 ± 0.0	2.0 ± 0.1		C 68.94% H 6.27% Cl 5.65% N 8.93% O 10.20%	C36H39ClN4O4	627.18963
A1B1C94_1	2.2 ± 0.1	8.3 ± 0.4		C 68.62% H 6.32% N 10.32% O 14.74%	C31H34N4O5	542.64043

A1B1C95_1	10.5 ± 0.3	8.3 ± 0.4		C 70.56% H 7.07% N 13.27% O 9.10%	C31H37N5O3	527.67224
A1B1C96_1	1.5 ± 0.0	2.6 ± 0.1		C 67.11% H 6.02% Cl 6.83% N 10.79% O 9.25%	C29H31ClN4O3	519.04842
A1B1C97_1	6.5 ± 0.2	4.7 ± 0.2		C 70.02% H 6.66% N 10.89% O 12.44%	C30H34N4O4	514.62988
A1B1C98_1	10.2 ± 0.3	8.6 ± 0.4		C 68.83% H 6.60% N 11.47% O 13.10%	C28H32N4O4	488.59164
A1B1C99_1	25.0 ± 0.6	8.3 ± 0.4		C 69.72% H 6.66% N 14.02% O 9.61%	C29H33N5O3	499.61806
A1B1C100_1	30.0 ± 0.8	9.0 ± 0.5		C 71.76% H 6.21% N 13.07% O 8.96%	C32H33N5O3	535.65151
A1B1C101_1	3.5 ± 0.1	0.8 ± 0.0		C 73.20% H 6.48% N 9.48% O 10.83%	C36H38N4O4	590.72866
A1B1C102_1	7.0 ± 0.2	3.2 ± 0.2		C 73.20% H 6.48% N 9.48% O 10.83%	C36H38N4O4	590.72866
A1B1C103_1	5.5 ± 0.1	5.4 ± 0.3		C 66.91% H 5.81% F 7.30% N 10.76% O 9.22%	C29H30F2N4O3	520.58425
A1B1C104_1	11.0 ± 0.3	7.5 ± 0.4		C 68.83% H 6.60% N 11.47% O 13.10%	C28H32N4O4	488.59164

A1B1C105_1	15.0 ± 0.4	5.0 ± 0.3		C 68.83% H 6.60% N 11.47% O 13.10%	C28H32N4O4	488.59164
A1B1C106_1	13.0 ± 0.3	5.1 ± 0.3		C 68.83% H 6.60% N 11.47% O 13.10%	C28H32N4O4	488.59164
A1B1C107_1	6.5 ± 0.2	3.6 ± 0.2		C 73.20% H 6.48% N 9.48% O 10.83%	C36H38N4O4	590.72866
A1B1C108_1	7.5 ± 0.2	5.0 ± 0.2		C 72.92% H 6.71% N 10.97% O 9.40%	C31H34N4O3	510.64163
A1B1C109_1	16.0 ± 0.4	7.6 ± 0.4		C 64.73% H 5.98% N 10.06% O 8.62%	C32H36N4O5	556.66752
A1B1C110_1	8.0 ± 0.2	6.2 ± 0.3		C 67.60% H 6.24% Cl 6.65% N 10.51% O 9.00%	C30H33ClN4O3	533.07551
A1B1C111_1	12.0 ± 0.3	18.9 ± 0.9		C 76.23% H 6.40% N 9.36% O 8.02%	C38H38N4O3	598.75156
A1B1C112_1	15.0 ± 0.4	7.9 ± 0.4		C 70.95% H 7.26% N 12.93% O 8.86%	C32H39N5O3	541.69933

A1B1C113_1	3.0 ± 0.1	7.1 ± 0.4		C 73.49% H 6.67% N 9.26% O 10.58%	C37H40N4O4	604.75575
A1B1C114_1	2.2 ± 0.1	1.4 ± 0.1		C 67.61% H 7.69% N 10.17% O 14.53%	C31H42N4O5	550.70419
A1B1C115_1	6.2 ± 0.2	0.8 ± 0.0		C 69.84% H 6.90% N 9.58% O 13.68%	C34H40N4O5	584.7217
A1B1C116_1	2.3 ± 0.1	12.8 ± 0.6		C 69.31% H 7.61% N 12.43% O 10.65%	C26H34N4O3	450.58588
A1B1C117_1	0.8 ± 0.0	15.8 ± 0.8		C 71.88% H 6.66% N 11.56% O 9.90%	C29H32N4O3	484.60339
A88B1C1_1	nt	8.2 ± 0.4		C 76.67% H 8.09% N 8.65% O 6.59%	C31H39N3O2	485.67538
A89B1C1_1	nt	99.0 ± *		C 68.70% H 7.79% N 8.66% O 9.89% S 4.96%	C37H50N4O4S	646.89945
A90B1C1_1	nt	2.6 ± 0.1		C 70.04% H 6.38% Cl 5.91% N 7.00% O 5.33% S 5.34%	C35H38ClN3O2S	600.22901
A91B1C119_0	nt	0.3 ± 0.0		C 73.34% H 6.81% F 4.14% N 12.22% O 3.49%	C28H31FN4O	458.58387

A1B1C118_1	nt	7.7 ± 0.4		C 72.41% H 7.17% N 8.66% O 7.42% Si 4.34%	C39H46N4O3Si	646.91247
A92B1C1_1	nt	0.9 ± 0.0		C 79.11% H 7.72% N 7.48% O 5.70%	C37H43N3O2	561.77416
A93B1C1_1	nt	2.6 ± 0.1		C 79.42% H 8.03% N 7.12% O 5.43%	C39H47N3O2	589.82834
A94B1C1_1	nt	99.0 ± *		C 72.81% H 6.26% Cl 5.24% N 6.21% O 4.73% S 4.74%	C41H42ClN3O2S	676.32779
A95B1C1_1	nt	2.7 ± 0.1		C 74.58% H 7.13% N 7.25% O 5.52% S 5.53%	C36H41N3O2S	579.81107
A1B1C120_1	nt	8.3 ± 0.4		C 71.20% H 7.24% N 10.06% O 11.50%	C33H40N4O4	556.71115

Supplementary Table 2. *In vitro* cytotoxicity of a subset of 114 compounds selected in the initial chemolibrary, measured by the IC50 (μM) on proliferating K-562 human erythroblasts. The subset corresponds to molecules inhibiting the *in vitro* proliferation of either *Toxoplasma gondii* or *Plasmodium falciparum* with an IC50 value lower or equal to 2 μM . IC50 values are based on two independent experiments, determined graphically from dose-effect curves, with indicated errors, using the Graphpad Prism analytical software.

compound identifier	IC50 K-562	compound identifier	IC50 K-562
A0B0C1_0	206.0 \pm 11.0	A23B1C1_1	169.0 \pm 8.5
A0B0C2_0	48.6 \pm 2.4	A24B1C1_1	144.0 \pm 7.2
A0B17C1_4	16.2 \pm 0.8	A25B1C1_1	90.5 \pm 4.5
A0B19C1_1	153.0 \pm 7.7	A27B1C1_1	1.4 \pm 0.1
A15B1C1_1	41.4 \pm 2.1	A29B1C1_1	20.5 \pm 1.0
A16B7C1_1	280.0 \pm 14.0	A30B1C1_1	82.3 \pm 4.1
A18B1C1_1	94.4 \pm 4.7	A31B1C1_1	14.4 \pm 0.7
A18B1C2_1	90.8 \pm 4.5	A34B1C1_1	20.0 \pm 1.0
A18B1C33_1	167.0 \pm 8.4	A35B1C1_1	26.0 \pm 1.3
A19B1C1_1	327.0 \pm 16.4	A38B1C1_1	9.5 \pm 0.5
A1B1C1_2	56.6 \pm 2.8	A38B1C2_1	15.2 \pm 0.8
A1B1C1_6	23.2 \pm 1.2	A3B1C1_1	394.6 \pm 19.7
A1B1C10_1	98.5 \pm 4.9	A41B1C2_1	8.4 \pm 0.4
A1B1C101_1	5.8 \pm 0.3	A43B1C1_1	107.0 \pm 5.4
A1B1C114_1	10.7 \pm 0.5	A44B1C1_1	162.0 \pm 8.1
A1B1C115_1	4.6 \pm 0.2	A45B1C1_1	298.0 \pm 14.9
A1B1C117_1	15.1 \pm 0.8	A46B1C1_1	141.0 \pm 7.1
A1B1C13_1	4.1 \pm 0.2	A47B1C1_1	177.0 \pm 8.9
A1B1C14_1	1.6 \pm 0.1	A48B1C1_1	143.0 \pm 7.2
A1B1C17_1	2.0 \pm 0.1	A51B1C1_1	13.3 \pm 0.7
A1B1C2_1	9.3 \pm 0.5	A53B1C2_1	159.0 \pm 7.9
A1B1C21_1	1.1 \pm 0.1	A58B1C1_1	114.0 \pm 5.7
A1B1C22_1	3.6 \pm 0.2	A5B3C0_0	97.2 \pm 4.7
A1B1C23_3	4.2 \pm 0.2	A5B3C1_1	22.4 \pm 1.1
A1B1C26_0	3.2 \pm 0.2	A63B1C1_1	24.6 \pm 1.2
A1B1C3_0	32.1 \pm 1.6	A64B1C1_1	138.0 \pm 6.9
A1B1C3_2	88.3 \pm 4.4	A65B1C1_1	21.3 \pm 1.1
A1B1C35_1	111.0 \pm 5.6	A68B1C1_1	268.0 \pm 13.4
A1B1C36_1	17.6 \pm 0.9	A69B1C1_1	334.0 \pm 16.7
A1B1C4_0	24.2 \pm 1.2	A6B1C1_1	5.3 \pm 0.3
A1B1C41_1	13.2 \pm 0.7	A70B1C1_1	280.0 \pm 14.0
A1B1C43_1	35.8 \pm 1.8	A70B1C2_1	83.5 \pm 4.2
A1B1C45_1	11.0 \pm 0.6	A71B1C1_1	204.0 \pm 10.2
A1B1C48_1	16.8 \pm 0.8	A71B1C2_1	143.0 \pm 7.2
A1B1C5_1	26.0 \pm 1.3	A72B1C1_1	78.6 \pm 3.9
A1B1C54_1	14.9 \pm 0.7	A73B1C1_1	87.7 \pm 4.4
A1B1C56_1	29.9 \pm 1.5	A74B1C1_1	202.0 \pm 10.1
A1B1C57_1	6.7 \pm 0.3	A74B1C2_1	32.9 \pm 1.7
A1B1C58_1	13.4 \pm 0.7	A77B1C1_1	36.0 \pm 1.8
A1B1C6_1	10.3 \pm 0.5	A79B1C1_1	44.2 \pm 2.2
A1B1C6_2	54.6 \pm 2.7	A7B1C1_1	55.0 \pm 2.8
A1B1C60_1	6.6 \pm 0.3	A7B1C2_1	25.3 \pm 1.3
A1B1C61_1	11.6 \pm 0.6	A82B1C1_1	99.0 \pm 4.9
A1B1C70_1	1.4 \pm 0.1	A83B1C1_1	90.9 \pm 4.6
A1B1C71_1	22.4 \pm 1.1	A84B1C1_1	113.0 \pm 5.6
A1B1C72_1	4.3 \pm 0.2	A87B1C1_1	74.2 \pm 3.7
A1B1C73_1	11.4 \pm 0.6	A8B1C1_1	151.6 \pm 7.6
A1B1C74_1	17.6 \pm 0.9	A9B1C1_1	17.0 \pm 0.8
A1B1C75_1	14.3 \pm 0.7		
A1B1C76_1	33.8 \pm 1.7		
A1B1C78_1	6.0 \pm 0.3		
A1B1C80_1	11.5 \pm 0.6		
A1B1C82_1	8.8 \pm 0.4		
A1B1C84_1	15.1 \pm 0.8		
A1B1C85_1	14.5 \pm 0.7		
A1B1C88_1	2.0 \pm 0.1		
A1B1C9_0	200.0 \pm 10.0		
A1B1C90_1	6.9 \pm 0.3		
A1B1C93_1	3.9 \pm 0.2		
A1B1C96_1	12.7 \pm 0.6		
A1B6C1_1	34.7 \pm 1.7		
A1B8C1_1	20.8 \pm 1.0		
A20B1C1_1	101.0 \pm 5.1		
A21B1C1_1	248.0 \pm 12.4		
A21B1C2_1	243.0 \pm 12.2		
A22B1C1_1	138.0 \pm 6.9		

Supplementary information 2
Preliminary proteomic study of possible targets of Piperidinyl-benzimidazolinone analogs in *Plasmodium falciparum*.

1. Methods. Affinity purification using a biotinylated analog

Preparation of the affinity matrix

One of the compounds, numbered A41B1C2_1 in the screened library and named here Biot-X is linked to a biotin group, circled in the following structure illustration:

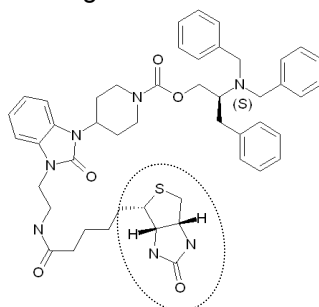


Figure I. Structure of Biot-X

We first linked Biot-X to a neutravidin-coupled affinity matrix (UltraLink Immobilized Neutravidin Protein Plus, Pierce) by the following procedure. A 2 mL stirred suspension of the neutravidin-matrix, corresponding to 1 mL of stabilized matrix, was washed 5 times with PBS (10 mL) and then incubated in presence of Biot-X (100 μ g of a suspension in DMSO, 5% w/v). After a 2 hour incubation at room temperature, the matrix was washed 5 times with the buffer used for protein extraction.

Preparation of protein samples

A culture of red blood cells infected by unsynchronized *P. falciparum* (3D7) cells or an equivalent quantity of uninfected red blood cells (mock) were collected using a benchtop centrifuge. An aliquot fraction of the obtained pellet was used to control parasitemia. Pellets were then suspended in RPMI 1640 medium (Roswell Park Memorial Institute medium, Gibco) containing saponin 0.05% to lyse red blood cells and re-centrifuged to discard the excess of hemoglobin released following red blood cell disruption. After washing twice in RPMI 1640, the pellet was subjected to a hypotonic lysis in presence of 10 volumes of water with an EDTA-free anti-protease mix (Sigma) and incubated 10 minutes in ice. After a 1 hour ultra-centrifugation at 100.000 x g, 4°C, the supernatant containing soluble proteins was collected. The pellet corresponding to membrane-enriched fractions was re-suspended in 3.5 mL extraction buffer 1 (10 mM Tris pH 7.4, 0.5% Triton X-100) and incubated for 30 minutes at room temperature. After a 1 hour ultra-centrifugation at 100.000 x g, 4°C, the supernatant containing proteins solubilized by Triton-X100 (Sigma-Aldrich) was collected. The pellet was re-suspended in 3.5 mL extraction buffer 2 (10 mM Tris pH 7.4, 0.5% Triton X-100, 1 M NDSB-201) and incubated for 30 minutes at room temperature. After a 1 hour ultra-centrifugation at 100.000 x g, 4°C, the supernatant containing proteins solubilized by Triton X-100 and the sulfobetain NDSB201 (3-(1-Pyridinio)-1-propanesulfonate, Fluka) was collected. Protein concentration was determined in all samples using the BCA kit (Uptima, Interchim).

Affinity chromatography

Prior to loading, 0.01 mg Streptavidin (Pierce) was added to all samples in order to block naturally biotinylated proteins and prevent their non-specific binding to the neutravidin-matrix. A 100 μ L aliquot fraction of all samples was kept for analysis. The affinity matrix coupled to Biot-X was mixed gently with protein samples in presence or absence of detergents and incubated 1 hour at room temperature. The mixture was then poured in a column (1 mL, height 2 cm) until complete sedimentation. The fraction of unbound proteins was eluted by addition of 1 mL of loading buffer and proteins were precipitated with TCA (trichloroacetic acid, Sigma), 10% at 4°C for 1 hour until analysis. The matrix was then washed with 10 mL of equilibration buffer (corresponding to the medium used to extract proteins) and then bound proteins were eluted with 4 mL diethylamine 1 M, pH 11.5 in extraction buffer. The pH of eluted fractions was immediately equilibrated with Tris-HCl 1 M, pH 7.4. Proteins were precipitated with TCA 10% at 4°C for 1 hour. Protein pellets obtained after TCA

precipitation were washed in ice-cold acetone. Distinct affinity matrices were used for the chromatography of infected and uninfected red blood cells.

Protein electrophoresis

Protein samples were mixed in loading buffer (Tris-HCl 50 mM, pH 6.8, glycerol 10% (v/v), SDS 1% (v/v), bromophenol blue 0.01% (v/v), DTT 25 mM), and analyzed by SDS-PAGE (polyacrylamide gel electrophoresis), using a 12% acrylamide (v/v) gel. Electrophoresis was run at constant voltage (200 V) in Tris 25 mM, glycine 0.192 M, pH 8.3, SDS 0.1% (v/v). The gel was stained with Coomassie brilliant-blue R250 (Sigma) by incubation for 30 min in acetic acid 10% (v/v), isopropanol 25% (v/v), Coomassie blue 2.5 g.L⁻¹.

Mass Spectrometry and Protein Identification.

After SDS PAGE, discrete spots were excised from the Coomassie blue-stained gel. An in-gel digestion was carried out as described (1, 2). Gel pieces were extracted with 5% (v/v) formic acid solution and acetonitrile. Extracted peptides were desalted using CapLC (Waters) reverse chromatography. Elution of peptides was performed with 5-10 µl of a 50:50:0.1 (v/v) acetonitrile/H₂O/formic acid solution. The tryptic peptide solution was introduced into a glass capillary (Protana, Odense, Denmark) for nanoelectrospray ionization. Tryptic peptides were assessed by electrospray ionization (ESI) and quadrupole time-of-flight mass spectrometry (ESI-Q-TOF; Ultima, Micromass) (1). Interpretation of spectra was achieved manually and with the help of the Mascot program (MatrixScience). Sequence information was used for database searching using the BLASTCOMP program performing BLAST searches for each amino acid sequence and clustering amino acid sequences identified from common BLAST hits. BLASTP was used to mine *P. falciparum* protein sequences via the PlasmoDB database.

2. Results. Detection of proteins from *P. falciparum* having an affinity for the piperidinyl-benzidazolidinone scaffold

The strategy to search target candidates is based on the affinity of the Biot-X compound for streptavidin on its biotinyl moiety and for the *P. falciparum* protein target on its target piperidinyl-benzidazolidinone moiety. A stepwise extraction of native soluble and membrane-associated proteins from *P. falciparum* was performed, following hypotonic lysis, solubilisation by Triton X-100 and by Triton X-100/ NDSB-201. Experiments were carried out using 4.5 mL pellets of infected red blood cells (parasitemia 5.2%; 2.3.10⁹ parasites). A pellet of uninfected red blood cells was used in a mock experiment run in parallel. The following table summarizes the amount of proteins used in each affinity chromatography.

	Soluble proteins (mg)	Proteins solubilised by Triton X-100 (mg)	Proteins solubilised by Triton X-100 / NDSB201 (mg)
RBC	0.707	0.973	0.721
Parasites	1.323	1.043	0.399

Table I. Protein fractions used for affinity chromatography

Each fraction was blocked by addition of Streptavidin and mixed with the Biot-X-Neutravidin-coupled matrix. Proteins bound to the matrix was eluted by addition of diethylamine 1 M, pH 11.5 and analyzed by SDS PAGE.

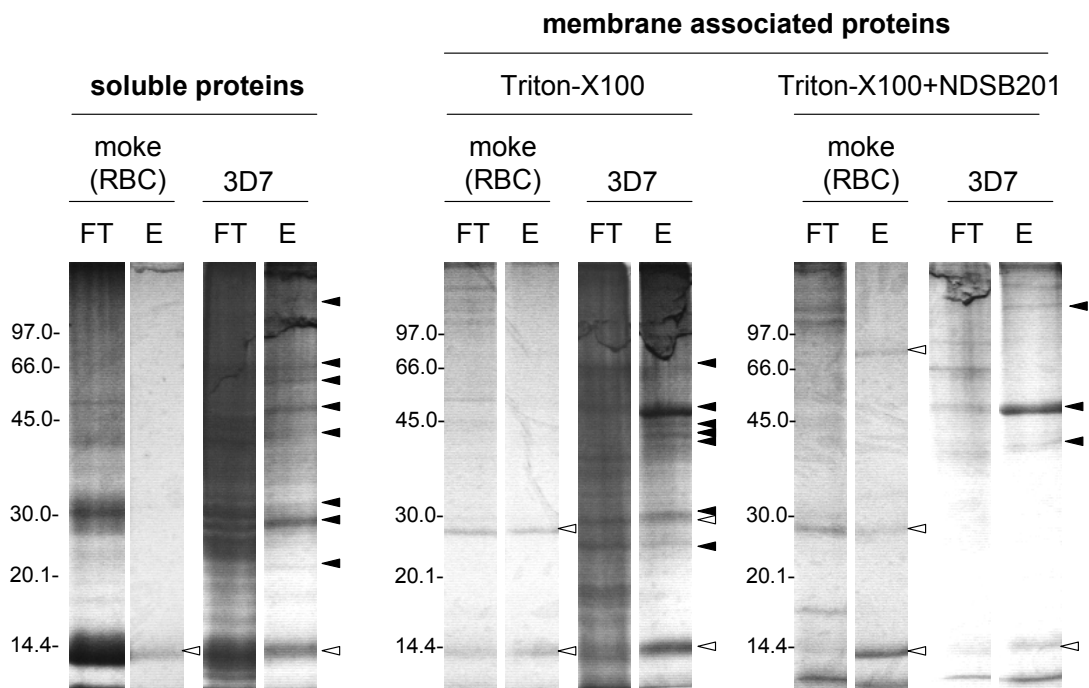


Figure II. SDS PAGE analysis of red blood cell (RBC) and *Plasmodium falciparum* polypeptides purified by affinity chromatography on a biotinylated piperidinyl-benzimidazolidinone analog. Proteins of uninfected (mock) and infected red blood cells were loaded on top of a Biot-X-Neutravidin affinity matrix. Unbound (flow through, FT) and bound (eluted, E) fractions were analyzed by SDS PAGE and stained with Coomassie blue. Main protein bands from parasite samples (black arrows) and from uninfected RBC (white arrows) were excised and analyzed by mass spectrometry

Protein bands visualised after Coomassie staining were excised and analyzed by mass spectrometry following the procedure described in the Method section. Red blood cell proteins that bind to the column consist of haemoglobin, a major contaminant and avidin tryptic peptides, either from the Streptavidin used to block protein samples or released by diethylamine from the affinity matrix.

Table II (following page). Mass spectrometry determination of major proteins from red blood cells and *Plasmodium falciparum* eluted from a chromatography affinity matrix coupled to a piperidinyl-benzimidazolidinone analog. The first part of the table shows polypeptides from uninfected red blood cells (mock) and the second part from *P. falciparum*. Since inhibitors might interfere with proteins interacting with nucleotides, lipids and 3-carbon glycerol substructures, the table also lists the corresponding interactions, including 3-carbon ligands such as glycerone-P, glyceraldehyde-3-P, lactate and pyruvate). Mito, mitochondria; ER, endoplasmic reticulum ; Rhop, rhoptries ; Sp, Signal peptide; Maurer structure.

Description of proteins corresponding to analyzed tryptic fragments		Accession	Organism	Score	Mass	Coverage	Number of tryptic peptides	Interaction with nucleotides	Interaction with lipids	Interaction with 3-carbon molecules	Trans-membrane domains	Compartment
Polypeptides characterized from uninfected red blood cells (mock)												
a	Hemoglobin subunit beta - <i>Homo sapiens</i> (Human)	HBB_HUMAN	Human	115,18	15988	17,24	3	-	-	-	-	cytoplasm
b	Avidin	-	-	268,50	16758	36,84	5	-	-	-	-	From the affinity matrix
Polypeptides characterized from red blood cells infected by <i>Plasmodium falciparum</i> 3D7												
1.	Merozoite surface protein 1, - <i>P. falciparum</i>	Q8I0J8_PLAF7 PF11475w	Plasmodium	872,86	195605	9,96	17	?	?	?	1	Sp; PM; MS
2.	High molecular weight rhoptry protein-2 - <i>P. falciparum</i>	Q8I060_PLAFA PF11445w	Plasmodium	862,45	162561	15,64	20	?	?	?	0 / 1	Sp; Rhop; MS
3.	Long-chain-fatty-acid-CoA ligase, putative - <i>P. falciparum</i>	Q8I535_PLAF7 PFL1880w	Plasmodium	517,18	92034	11,84	8	AMP/ ATP	Acyl-CoA		0	cytoplasm
4.	Heat shock 70 kDa protein - <i>P. falciparum</i>	Q8IB24_PLAF7 PF08_0054	Plasmodium	993,86	73868	28,76	15	ATP			0	Cytoplasm; Mito; MS
5.	Heat shock protein - <i>P. falciparum</i>	Q8I2X4_PLAF7 PFI0875w	Plasmodium	1073,3	72343	32,88	19	ATP			0	Sp; ER; MS
6.	Putative uncharacterized protein - <i>P. falciparum</i>	Q8IIV8_PLAF7 PF11_0055	Plasmodium	639,74	49235	29,75	13	NADP?	?	?	0	Sp; MS apicoplast; ER?
7.	Putative pyruvate kinase - <i>P. falciparum</i>	Q6LF06_PLAF7 PFF1300w	Plasmodium	997,75	55625	43,96	15	ATP		pyruvate	0 / 1	Cytoplasm; MS
8.	Elongation factor 1-alpha - <i>P. falciparum</i>	Q8I0P6_PLAF7 PF13_0304	Plasmodium	916,01	48928	45,05	16	GTP			0	Cytoplasm; MS
9.	Fructose-bisphosphate aldolase - <i>P. falciparum</i>	ALF_PLAFA PF14_0425	Plasmodium	402,88	40080	24,66	7			glycerone-P + glyceraldehyde 3-P	0	Cytoplasm; MS
10.	L-lactate dehydrogenase - <i>P. falciparum</i>	LDH_PLAFD PF13_0141	Plasmodium	352,08	34086	20,65	6	NAD		D-lactate ; pyruvate	0	Sp+Tp; MS apicoplast
11.	Adenylate kinase 2 - <i>P. falciparum</i>	Q7Z0H0_PLAFA PF10_0086	Plasmodium	425,39	27594	38,80	8	ATP			0	Cytoplasm; MS
12.	Putative Rab7 GTPase - <i>P. falciparum</i>	Q9NFG0_PLAFA PFI0155c	Plasmodium	274,00	23773	26,85	5	GTP/ ATP			0	Sp; Nucleus ?

In the list of the 12 most abundant proteins interacting with Biot-X, some polypeptides are likely contaminants, such as MSP-1 (Merozoite Surface Protein 1), RhopH2 (High Molecular Weight Rhoptry Protein) or Heat shock proteins and LDH (Lactate dehydrogenase). The Long-chain-fatty-acid-CoA ligase (PlasmoDB PFL1880w) might bind Biot-X due to its action on a fatty acyl substrate. Other protein candidates might be inhibited by interference with their interaction with a 3-carbon scaffold close to glycerol. Future functional studies shall be performed to refine the effects of the interaction of these protein target candidates with active piperidiny-benzimidazolidinone analogs, including other minor proteins also detected by mass spectrometry.

References

1. **Ferro, M., D. Salvi, H. Riviere-Rolland, T. Vermat, D. Seigneurin-Berny, D. Grunwald, J. Garin, J. Joyard, and N. Rolland.** 2002. Integral membrane proteins of the chloroplast envelope: Identification and subcellular localization of new transporters. *Proc Natl Acad Sci U S A* **99**:11487-11492.
2. **Ferro, M., D. Seigneurin-Berny, N. Rolland, A. Chapel, D. Salvi, J. Garin, and J. Joyard.** 2000. Organic solvent extraction as a versatile procedure to identify hydrophobic chloroplast membrane proteins. *Electrophoresis* **21**:3517-3526.